haematologica
Journal of the Ferrata Storti Foundation

NLRP6 regulates donor T cell activation and acute graft-*versus*-host disease *via* ZAP-70-Erk pathway

by Eri Matsuki, Masahiro Miyata, Ryo Sato, Jana Gawron, Masahiro Suto, Hiroya Tamaki, Hideaki Fujiwara, Ai Ito, Tsunekazu Hishima, Yuki Ishizawa, Erika Sekiguchi, Tayu Tobai, Sae Ushio, Katherine Oravecz-Wilson, Grace Chen, Isao Tawara, Kazunobu Ichikawa, Masafumi Watanabe, Kenichi Ishizawa, Hisayuki Yokoyama, Daniel Peltier, Bruce Blazar, Robert Zeiser, Pavan Reddy and Tomomi Toubai

Received: September 13, 2025.
Accepted: June 22, 2026.

Citation: Eri Matsuki, Masahiro Miyata, Ryo Sato, Jana Gawron, Masahiro Suto, Hiroya Tamaki, Hideaki Fujiwara, Ai Ito, Tsunekazu Hishima, Yuki Ishizawa, Erika Sekiguchi, Tayu Tobai, Sae Ushio, Katherine Oravecz-Wilson, Grace Chen, Isao Tawara, Kazunobu Ichikawa, Masafumi Watanabe, Kenichi Ishizawa, Hisayuki Yokoyama, Daniel Peltier, Bruce Blazar, Robert Zeiser, Pavan Reddy and Tomomi Toubai. NLRP6 regulates donor T cell activation and acute graft-versus-host disease via ZAP-70-Erk pathway.
Haematologica. 2026 July 2. doi: 10.3324/haematol.2025.289144 [Epub ahead of print]

Research article

NLRP6 regulates donor T cell activation and acute graft-*versus*-host disease via ZAP-70-Erk pathway

Eri Matsuki[1#], Masahiro Miyata[1#], Ryo Sato[2#], Jana Gawron[3,4], Masahiro Suto[5], Hiroya Tamaki[6], Hideaki Fujiwara[7], Ai Ito[8], Tsunekazu Hishima[8], Yuki Ishizawa[2], Erika Sekiguchi[9], Tayu Tobai[10], Sae Ushio[11], Katherine Oravecz-Wilson[12], Grace Chen[13], Isao Tawara[14], Kazunobu Ichikawa[1], Masafumi Watanabe[1], Kenichi Ishizawa[2], Hisayuki Yokoyama[2], Daniel Peltier[15], Bruce Blazar[16], Robert Zeiser[3], Pavan Reddy[17], Tomomi Toubai[2,18*]

[1]Department of Internal Medicine I, Yamagata University Faculty of Medicine, Yamagata, Japan. [2]Department of Internal Medicine III, Division of Hematology and Cell Therapy, Yamagata University Faculty of Medicine, Yamagata, Japan. [3]Department of Medicine I, Faculty of Medicine, University of Freiburg, Freiburg, Germany. [4]Faculty of Biology, Albert-Ludwigs University, Freiburg, Germany.[5]Department of Pharmaceutical Science, Yamagata University Faculty of Medicine, Yamagata, Japan. [6]Division of Hematology, Department of Internal Medicine, Hyogo College of Medicine, Nishinomiya, Japan. [7]Department of Hematology and Oncology, Okayama University Hospital, Okayama, Japan. [8]Departmemt of Pathology, Tokyo Metropolitan Cancer and Infectious Diseases Center Komagome Hospital, Tokyo, Japan. [9]Keio University Hospital, Shinjuku, Japan. [10]Case Western Reserve University, Cleveland, OH, USA. [11]Yamagata University Faculty of Medicine, Yamagata, Japan.[12]Department of Internal Medicine, Division of Hematology and Oncology, University of Michigan Rogel Cancer Center, Ann Arbor, MI, USA. [13]Department of Internal Medicine, Division of Gastroenterology, University of Michigan Comprehensive Cancer Center, Ann Arbor, MI, USA.[14]Department of Hematology and Oncology, Mie University Graduate School of Medicine, Tsu, Japan. [15]Department of Pediatrics, Department of Microbiology and Immunology, Division of Hematology Oncology and Stem Cell Transplantation, Simon Comprehensive Cancer Center, Indiana University, Indianapolis, IN, USA.[16]Department of Pediatrics, Division of Blood & Marrow Transplant & Cellular Therapy, University of Minnesota, Minneapolis, MN, USA. [17]Baylor Cancer Center, Houston, TX, USA. [18]Clinical Research and Trial Center, Tokyo Metropolitan Cancer and Infectious Diseases Center Komagome Hospital, Tokyo, Japan.

[#] These authors contributed equally to this work.

Short title: NLRP6 regulates T cell activation

Keywords: NLRP6, donor T cells, graft-versus-host disease, ZAP-70-Erk signaling

*Corresponding Author:

Tomomi Toubai

Clinical Research and Trial Center, Tokyo Metropolitan Cancer and Infectious Disease Center Komagome Hospital, 3-18-22 Honkomagome, Bunkyo-City, Tokyo, 113-8677, Japan.

E-mail: toubai@med.id.yamagata-u.ac.jp

Tel: +81-3-3823-2101

Conflict of interest statement

The authors have no conflict of interest.

Author contributions

EM designed and performed experiments, analyzed the data and wrote the paper. MM and RS: designed and performed experiments, analyzed the data and wrote the paper. JG, MS, HT, and HF: performed experiments and analyzed data. AI and TS analyzed pathological samples. YI, ES, TT, and SU: performed experiments. KOW: contributed reagents. GC and IT: contributed reagents and critically reviewed. MW, KI, and HY: provided advise on the experimental design. DP, and BB: critically reviewed and edited the manuscript. RZ, and PR: designed experiments, analyzed the data and critically reviewed and edited the manuscript. TT designed and performed experiments, analyzed the data and wrote the paper.

Acknowledgments

This work was supported by the Ministry of Education, Science, Sports, and Culture, Japan, Grant-in-Aid for Scientific Research (C) Grant Number JP20K08704, JP23K07850 (TT), The Japanese Society of Hematology Research Grant (TT), , an Amy Strelzer Manasevit Research Program grant which is funded through the Be the Match Foundation® (DP), and start-up funds from the Indiana University School of Medicine, Riley Children's Foundation and Melvin and Bren Simon Comprehensive Cancer Center (DP).

DATA Availability Statement

The data that support the findings of this study are available on request from the corresponding author: toubai@med.id.yamagata-u.ac.jp. The data are not publicly available due to privacy or ethical restrictions.

ABSTRACT

NOD-like receptor family pyrin domain-containing 6 (Nlrp6) is an inflammasome related molecule expressed in intestinal epithelial and immune cells. While previous work showed that Nlrp6 in host non-hematopoietic cells exacerbates gastrointestinal acute graft-versus-host disease (aGVHD), its role in donor T cells remained unclear. Here we show that donor T cell-intrinsic Nlrp6 exerts a protective effect in murine aGVHD models. Mice receiving Nlrp6 deficient (*Nlrp6*$^{-/-}$) donor T cells had reduced survival and more severe GVHD than those receiving wild-type T cells. Mechanistically, *Nlrp6*$^{-/-}$ T cells showed enhanced proliferation, preferential Th1 differentiation, and upregulation of Th1 cytokines. Enhanced phosphorylation of Zap-70 and Erk1/2 indicated hyperactivation of proximal TCR signaling. Despite increased aGVHD, graft-versus tumor (GVT) responses preserved in *Nlrp6*$^{-/-}$ T cells. Clinically, T cells from aGVHD patients showed decreased Nlrp6 expression, supporting the relevance of our findings. Collectively, these data suggest that Nlrp6 negatively regulates allogeneic donor T cell responses, via Zap-70-Erk1/2 signaling, while sparing anti-tumor immunity. We conclude that beneficial effects of Nlrp6 expression in donor T cells opposes the detrimental Nlrp6 effects in intestinal epithelial cells during aGVHD indicating Nlrp6 has cell type-specific and context-dependent antagonistic biological functions on controlling aGVHD inflammatory responses.

INTRODUCTION

Acute graft-versus-host disease (aGVHD) is a life-threatening complication of allogeneic hematopoietic cell transplantation (allo-HCT). Donor T cells are necessary for the development of aGVHD[1] but are also critical for the graft-versus-tumor (GVT) effect, which can be curative for hematological malignancies[1]. Current immunosuppressive drugs targeting allogeneic T cell activation tend to inhibit not only GVHD but also GVT. Therefore, developing therapies that prevent GVHD while preserving GVT may improve allo-HCT outcomes.

The innate immune receptor nucleotide-binding oligomerization domain (NOD)-like receptor family pyrin domain-containing 6 (Nlrp6), is widely expressed in bone marrow-derived immune cells[2] as well as in the intestinal tract[3, 4], liver[5], kidney[6], and nervous system[7]. The conditioning regimen and aGVHD-induced tissue injury cause the release of damage-associated molecular patterns (DAMPs) and pathogen associated molecular patterns (PAMPs) that are detected by and result in the formation of a multiprotein complex termed the inflammasome. Upon recruitment of the adaptor protein apoptosis-associated speck-like protein (ASC), the inflammasome activates caspase-1 and caspase-11, that in turn cleaves the precursors of the inflammatory cytokines IL-18 and IL-1β into their active mature forms.

Within the intestinal tract, Nlrp6 is expressed in intestinal epithelial cells where it maintains intestinal homeostasis by regulating mucus secretion, tissue regeneration and the microbiome. In murine models, the intestinal Nlrp6 inflammasome suppresses inflammatory bowel disease, inflammation-related colorectal cancer and hepatocellular carcinoma [4, 5, 8]. In addition, Nlrp6 regulates bacterial and viral infections through both inflammasome-dependent and -independent mechanisms[9]. In contrast to its protective role in inflammation-associated tumorigenesis and colitis, Nlrp6 expression in intestinal epithelial cells exacerbates aGVHD[10]. Furthermore, the Nlrp6 inflammasome is not required for baseline colonic inner mucus layer formation or function in *Nlrp6*$^{-/-}$ mice [11-13]. Collectively, these recent studies suggest Nlrp6 has inflammasome-dependent and -independent functions that vary according to the environmental context.

Nlrp6 is also expressed in immune cells. In neutrophils, Nlrp6 negatively regulates their recruitment and function during *Streptococcus pneumoniae* infection[14]. In inflammatory monocytes, it is important for

promoting intestinal repair[11], and in colorectal cancer it enhances monocytic myeloid-derived suppressor cells (MDSCs) thereby increase metastasis[13]. In CD4+ T cells, Nlrp6 deficiency has been reported to decrease T cell survival, increase T cell death, and reduce IFN-γ production of *in vitro* differentiated type 1 helper (Th1) cells in an inflammasome-independent manner[15]. These data suggest that innate and adaptive immune system function is influenced by Nlrp6 via both inflammasome-dependent and -independent mechanisms. Since the role of Nlrp6 in donor T cells after allo-HCT is unknown, we tested the donor T cell-intrinsic effect of Nlrp6 expression in murine models of allo-HCT. Surprisingly, we found that Nlrp6$^{-/-}$ donor T cells exacerbate aGVHD whereas we previously found that Nlrp6 deficiency in non-hematopoietic host tissues protected against aGVHD[10]. Mechanistically, we found donor T cell intrinsic Nlrp6 deficiency enhanced T cell activation and proliferation after allogeneic stimulation that was associated with an augmentation of the Zap-70-Erk1/2 signaling pathway. Collectively, our results highlight the cell type-specific, divergent effects of Nlrp6 on aGVHD.

METHODS

Detailed procedures are described in the supplemental methods.

Mice

C57BL/6 (B6, H-2^{b}), BALB/c (H-2^{d}), B6D2F1 (H-2$^{b/d}$) and B10.BR (H-2^{k}) mice were purchased from vendors. C3H.sw and B6 background NLRP6 knock-out (B6-*Nlrp6*$^{-/-}$) mice were provided by collaborators[4]. All experiments were approved by local institution animal care and use Committees.

In vitro T cell stimulation

CD90.2+ T cells were stimulated with anti-CD3 (1μg/ml) and -CD28 (1μg/ml) antibodies for various amounts of time.

Bone Marrow Transplantation

BMTs were performed as previously described[16, 17]. Briefly, donor splenic T cells were enriched and bone marrow T cells were depleted by MACS (Miltenyi Biotec). Recipients were irradiated with various doses on day –1 and injected with T cells along with 5×10^{6} T cell-depleted bone marrow (TCD-BM) cells from either syngeneic or allogeneic B6-WT or B6-*Nlrp6*$^{-/-}$ donors on day 0[18]. Survival was recorded daily and body weight and systemic aGVHD clinical scores were measured weekly. Histopathological

analysis of gastrointestinal (GI) tract which is the primary acute GVHD target organ, was performed on day 14 as described previously utilizing a semiquantitative scoring system implemented by two blind reviewers[19].

Post allo-HCT analysis

On days 7 and 14, spleens were removed from BMT mice and analyzed for donor T cell functions.

Mixed lymphocyte reaction (MLR)

Splenic T cells were co-cultured with BMDCs used as stimulators in an MLR.

T cell proliferation assay with BrdU incorporation

Proliferation was assessed using the CFSE cell division tracker kit and BrdU Flow Kit, following the manufacturer's protocol.

Flow cytometry

Flow cytometry was performed as previously described[10, 20, 21]. Both cell surface and intracellular staining were performed using appropriate antibodies. TCR signaling kinetics were assessed by phospho-flow and Western blotting (Zap-70, pZAp-70, Erk1/2, pErk1/2). The ERK inhibitor FR180204 was used during stimulation.

Cytokine ELISA

Serum and culture supernatant levels of TNF and IFN-γ were measured using BD OptEIA (BD Biosciences).

T cell differentiation and Treg suppression assay

Naïve CD4+ T cells were polarized into Th1, Th2, or Th17 subsets using commercially available kits. The Treg suppression assay was performed by co-culturing conventional (CD4+CD25-) and regulatory (CD4+CD25+) T cells together with BMDCs.

Western blot analysis

T cells were lysed in radio-immunoprecipitation assay (RIPA) buffer and total proteins was extracted as previously reported[18, 22].

In vivo imaging of the GVT effect

In vivo GVT effect was assessed using the IVIS imaging system.

Cytotoxic T lymphocyte (CTL) assay

CTL assay was evaluated against target tumor cells and quantified by Annexin V staining.

Spectral flow from human PBMCs

PBMCs were isolated and stained with multicolor antibody panels. The studies were approved by the Institutional Ethics Review Board of the Medical Center of the University of Freiburg, Germany (protocol no: 22-1047). Patient characteristics are listed in supplemental Table1.

Statistical analysis

Data are presented as mean ±SEM. Statistical significance was determined using the Mann–Whitney U-test or unpaired T-test. Survival data were analyzed using the Log-rank test.

RESULTS

T cell Nlrp6 expression increases early after stimulation.

We first confirmed Nlrp6 expression in murine T cells, then examined its expression following *in vitro* T cell activation using anti-CD3 and -CD28 antibodies. Following activation, Nlrp6 mRNA expression increased within 1-3 hours (**Supplemental Figure 1a**) and the expression of Nlrp6 in both CD4+ T and

CD8+ T cells were increased (**Supplemental Figure 1b-d**). These data demonstrated the dynamic expression of Nlrp6 following T cell activation opening up the possibility that Nlrp6 may be an important regulator of T cell responses.

Nlrp6$^{-/-}$ donor T cells exacerbate acute GVHD independent of conditioning-induced DAMPs

To determine if Nlrp6 regulates allogeneic T cell responses following allo-HCT, we assessed whether T cell development was altered in C57BL/6 (B6) *Nlrp6*$^{-/-}$ mice as compared to B6 wild-type (WT) mice. We found that the number of CD8+ T cells as well as CD4+ central memory and CD8 naïve T cell subsets in *Nlrp6*$^{-/-}$ mice were statistically, albeit modestly, less than WT mice (**Supplemental Figure 2a-h**). Thus, T cell development is minimally impacted in *Nlrp6*$^{-/-}$ mice as published elsewhere[15].

We previously showed that Nlrp6 deficiency in non-hematopoietic host tissues protected against aGVHD[10]. Others demonstrated that *Nlrp6*$^{-/-}$ T cells were less inflammatory and more susceptible to cell death[15]. Thus, we hypothesized that Nlrp6 expression could contribute to aGVHD pathogenesis and that *Nlrp6*$^{-/-}$ donor T cells would ameliorate aGVHD. To test this, recipient BALB/c mice were transplanted with either syngeneic BALB/c or allogeneic major histocompatibility complex (MHC) mismatched B6 WT bone marrow (BM) supplemented with syngeneic BALB/c, allogeneic B6 WT, or allogeneic B6 *Nlrp6*$^{-/-}$ donor T cells. Contrary to our hypothesis, the survival of allogeneic recipients receiving *Nlrp6*$^{-/-}$ donor T cells was significantly worse than those receiving WT T cells (**Figure 1A**). Similar results were obtained using an MHC mismatched B6 into B10.BR model (**Supplemental Figure 3**) and a haploidentical B6 into B6D2F1 model (**Figure 1C**). Consistent with acute GVHD driving the differences observed in mortality, acute GVHD histopathology scores in the small and large trended higher in recipients of *Nlrp6*$^{-/-}$ T cells (**Figure 1E**). Because we wanted to confirm whether Nlrp6 in donor T cells regulates GVHD severity and mortality independent of environmental factors, we utilized the same models as described above but performed these studies at both Yamagata University (Japan) and the University of Michigan (USA). We found that aGVHD-related morbidity and mortality were worse in allogeneic recipients of *Nlrp6*$^{-/-}$ T cells at both institutions (**Figure 1A-D**). These data suggested that the ability of Nlrp6 in donor T cells to ameliorate aGVHD was not specific to an individual breeding environment.

Nlrp6 plays an essential role in the inflammasome-mediated immune response to DAMPs[3, 4]. To determine whether conditioning-related tissue damage was required for less severe aGVHD observed following transfer of WT relative to *Nlrp6*$^{-/-}$ donor T cells, we used a conditioning-free B6 into B6D2F1 aGVHD model. Similar to the models above that used radiation-based conditioning, we found that aGVHD-related mortality in the conditioning-free model was worse in allogeneic recipients of *Nlrp6*$^{-/-}$ donor T cells compared to recipients of WT donor T cells (**Figure 1F**). Thus, conditioning-related tissue damage was not required for the more severe aGVHD induced by allogeneic *Nlrp6*$^{-/-}$ donor T cells.

T cell expansion and IFN-γ production are increased in allogeneic Nlrp6$^{-/-}$ donor T cells.

To determine the cellular mechanisms for why B6 *Nlrp6*$^{-/-}$ donor T cells caused more severe aGVHD, we examined the expansion and activation of donor T cells in BALB/c recipients after allo-BMT. In the spleen on day 7, CD4+ and CD8+ donor T cell expression of activation (CD69, CD25) and exhaustion (Tox, Tim-3) markers were increased, whereas in the spleen on day 14, total and CD4+ donor T cell numbers were significantly increased in recipients receiving *Nlrp6*$^{-/-}$ compared to WT donor T cells (**Figure 2A-B, Supplemental Figure 4a-e**). At both time points, significantly higher numbers of donor splenic *Nlrp6*$^{-/-}$ vs WT CD8+ and CD4+ T cells expressed TOX (**Figure 2B**) and were IFN-γ-producing (**Figure 2C**).

These increased CD4+ IFNγ+T cells tend to have high expression of T-bet (**Supplemental Figure 4f**). Therefore, Nlrp6 in activated T cells may regulate Th1 priming. In addition, these CD4+ IFN-γ+ T cells also co-expressed high levels of TOX (**Figure 2D**). Consistent with their propensity for heightened activation, early apoptotic (annexin V+ propidium iodide (PI)-) T cells likely indicative of increased activation induced cell death, were increased in *Nlrp6*$^{-/-}$ donor T cells (**Figure 2E**). These data suggest that Nlrp6 regulates allogeneic T cell expansion, apoptosis, and exhaustion early post- allo-BMT. Notably, serum TNF-α and regulatory T cells, IL-17A producing CD4+ and CD8+ T cells were unaffected (**Supplemental Figure 4g-i)** as were the inflammasome-associated cytokines IL-1β and IL-18 (data not shown). We also examined donor T cell expansion in mesenteric lymph nodes and liver and found a trend for an increased absolute number of donor T cells in the liver (**Figure 2F**, **Supplemental Figure 4j-l).** Altogether, these data suggest that Nlrp6 in activated donor T cells regulates allogeneic donor T cell expansion, exhaustion, apoptosis, and IFN-γ production while inflammasome-related cytokine production remains unchanged.

***Nlrp6*$^{-/-}$ T cell responses are increased after allogeneic and non-specific TCR stimulation.**

To determine the cell-intrinsic effect of Nlrp6 in allogenic donor T cells, we measured proliferation and cytokine production in mixed lymphocyte reactions (MLR) and following non-specific TCR stimulation with anti-CD3 and -CD28 antibodies *in vitro*. Consistent with increased aGVHD severity and expansion of donor allogeneic *Nlrp6*$^{-/-}$ donor T cells *in vivo*, thymidine incorporation was increased in *Nlrp6*$^{-/-}$ T cells compared to WT T cells after both in vitro MLR (day 5) and non-specific TCR stimulation (day 1,2) (**Figure 3A-B**). IFN-γ production (days 4,5) and cell division (day 5), indicated by CFSE dilution, were also increased in allo-stimulated *Nlrp6*$^{-/-}$ T cells (**Figure 3C-D**). Next, we measured DNA synthesis by BrdU incorporation and found that following non-specific stimulation BrdU incorporation for the last 16 hours on day 3 was increased in both CD4+ and CD8+ T cells from *Nlrp6*$^{-/-}$ T cells (**Figure 3E**). Because Nlrp6 can function as an inflammasome component, we also tested whether caspase inhibition altered T cell proliferation in *Nlrp6*$^{-/-}$ T cells but found no effect (**Supplemental figure 5**). Collectively, these data show that Nlrp6 negatively regulates T cell proliferation, cellular division, DNA synthesis, and inflammatory cytokine production following allogeneic or non-specific TCR stimulation.

Nlrp6 regulates allogeneic donor T cell-mediated aGVHD.

While the number of haploidentical and MHC mismatched HCTs have been increasing in recent years, MHC-matched related and unrelated HCTs are still the most common donor types. To determine whether Nlrp6 expression in donor T cells ameliorated aGVHD in the absence of any MHC mismatch, we used the B6 into C3H.sw MHC-matched, multiple minor histocompatibility antigen mismatched murine model of aGVHD. Surprisingly, survival of allogenic recipients of *Nlrp6*$^{-/-}$ donor T cell was equivalent to that of WT T cells (**Figure 4A**). Apart from differences in MHC and minor histocompatibility matching, the B6 into C3H.sw aGVHD model differs from our main MHC mismatched models, B6 into BALB/c and B6 into B6D2F1, by primarily being driven by allogeneic CD8+ rather than CD4+ T cells[23]. In CD4+ T cells, Nlrp6 promotes survival, pErk1/2 expression, and Th1 differentiation and cytokine production[15]. However, to our knowledge, its role in CD8+ T cells is unknown. Therefore, we hypothesized that Nlrp6 may preferentially drive CD4+ allogeneic T cell responses in which case B6 *Nlrp6*$^{-/-}$ T cells would not cause more severe GVHD than WT T cells in the B6 into C3H.sw model that is dominated by allogeneic CD8+ T cell effects. To test this hypothesis, purified CD4+ and/or CD8+ T cells from B6 WT or *Nlrp6*$^{-/-}$ donors were transplanted into irradiated C3H.sw recipients. GVHD mortality was enhanced only when purified B6-*Nlrp6*$^{-/-}$ CD4+ but not CD8+ T cells were given (**Figure 4B-C**). To eliminate strain- dependent factors and determine whether Nlrp6 expression negatively regulates CD4+ but not CD8+ T cell-mediated aGVHD in an MHC mismatched model, we transplanted purified CD4+ or CD8^{+} T cells from B6 WT and *Nlrp6*$^{-/-}$ donors into BALB/c recipients. As observed in the CD8+ T cell-

dominated B6 into C3H.sw GVHD model, the survival of BALB/c recipients receiving B6 *Nlrp6*$^{-/-}$ donor T cells was significantly worse than those receiving B6 WT donor T cells only when CD4+ and not CD8+ T cells were transplanted (**Figure 4D-E**). These data indicated that Nlrp6 expression in donor T cells may be beneficial for modulating aGVHD, especially CD4+ T cell-mediated allogeneic responses.

Nlrp6 inhibits *in vitro* Th1 differentiation.

Increased Th1 and Th17 polarization of CD4+ allogeneic donor T cells is associated with worse aGVHD[1]. Because only B6 CD4+ *Nlrp6*$^{-/-}$ T cells enhanced GVHD, we tested whether Nlrp6 regulates helper T cell differentiation into Th1, Th2, and Th17 subsets. Consistent with our *in vivo* data, T-bet expression and Th1 *in vitro* differentiation were enhanced in B6 *Nlrp6*$^{-/-}$ T cells (**Figure 5A**). By contrast, Th2 and Th17 differentiation were not altered by Nlrp6 (**Figure 5B-C**). It is possible that Nlrp6 might augment CD4+CD25+ regulatory T cell (Tregs) function thereby contributing to the more severe aGVHD caused by *Nlrp6*$^{-/-}$ allogeneic donor T cells. To determine if Nlrp6 could regulate Treg function, we performed an *in vitro* Treg suppression assay and found that *Nlrp6*$^{-/-}$ Tregs were equally as suppressive as WT Tregs (**Figure 5D**). Altogether, these results indicated that the absence of Nlrp6 increases Th1 polarization which may contribute to more severe aGVHD caused by *Nlrp6*$^{-/-}$ CD4+ allogenic T cells.

Nlrp6 regulates the Zap-70-Erk pathway.

To determine the molecular mechanisms underlying Nlrp6 regulation of T cells, we tested whether Nlrp6 influenced TCR signal transduction pathways. We focused on downstream activation of Zap-70 and Erk because they enhance Th1 differentiation[24-28]. After non-specific TCR stimulation as measured by flow cytometry, the expression of unphosphorylated Zap-70 protein at 24 hours decreased more in *Nlrp6*$^{-/-}$ compared to WT CD4+ T cells, suggesting that active phosphorylated Zap-70 (pZap-70) increased in *Nlrp6*$^{-/-}$ compared to WT CD4+ T cells (data not shown). Therefore, we next examined Zap-70 phosphorylation by western blotting and found that pZAP-70 indeed was enhanced in non-specifically activated *Nlrp6*$^{-/-}$ T cells (**Supplemental Figure 6a, c**). Erk activation is downstream of Zap-70 in the TCR pathway[29], and this pathway is enhanced by the absence of Nlrp6 in cells other than T cells[7, 30, 31]. Hence, we examined the phosphorylation of Erk and found that the expression of phosphorylated Erk1/2 was increased in *Nlrp6*$^{-/-}$ CD4+ and CD8+ T cells stimulated for 6 hours with anti-CD3/CD28 antibodies (**Supplemental Figure 6b, d**). We also found that Erk phosphorylation two and five minutes

after T cell stimulation was enhanced in *Nlrp6*$^{-/-}$ CD4+ T cells (**Figure 6A-B**, **Supplemental Figure 6e**). These data are consistent with previous work showing that phosphorylation of Erk1/2 is important for allogeneic T cell activation in aGVHD[32]. Importantly, there was no difference in the phosphorylation of Lck (**Supplemental Figure 7a**) in *Nlrp6*$^{-/-}$ T cells, indicating that Nlrp6 deficiency did not globally alter TCR signaling. Since the phosphorylation of Stat3 in T cells is also associated with GVHD[32], we examined Stat3 phosphorylation and found no difference between WT and *Nlrp6*$^{-/-}$ T cells (**Supplemental Figure 7b**).

To further test whether the ZAP-70-Erk pathway was necessary for enhanced activation of *Nlrp6*$^{-/-}$ T cells, we treated *Nlrp6*$^{-/-}$ and WT T cells with an Erk kinase inhibitor. We found that the Erk inhibitor reduced Erk signaling in both *Nlrp6*$^{-/-}$ and WT T cells, however, a significant decrease in CD4+ T cells was more consistently observed under in *Nlrp6*$^{-/-}$ T cells under various conditions, including different inhibitor concentrations and at both 2 and 5 minutes after stimulation. (**Figure 6C, Supplemental Figure 6f-g**). Collectively, our results suggested that the dampening of ZAP-70-Erk signaling following T cell activation by Nlrp6 is s more pronounced and consistent in CD4+ T cells.

***Nlrp6*$^{-/-}$ T cells maintain GVT responses.**

Allogeneic T cell-mediated aGVHD and GVT responses are tightly linked[1], making it difficult to target aGVHD without increasing the risk for relapse. CD8+ cytolytic activity is critical for GVT responses[33]. With this in mind, we were intrigued when CD8+ donor T-cell expansion, activation, and cytokine production 7 days after allo-BMT (**Figure 2B-D, Supplemental Figure 2b, d-e**) as well as proliferation after non-specific TCR stimulation (**Figure 3E**) were increased in *Nlrp6*$^{-/-}$ T cells, yet Nlrp6 deficiency did not affect CD8+ T cell-mediated aGVHD-related mortality (**Figure 4C, E**). Thus, we hypothesized that Nlrp6 would not influence GVT responses. To test this, we determined whether deficiency of Nlrp6 in allogeneic T cells altered their anti-leukemia activity. For this, we used the B6 into BALB/c model described above but added Baf/3-ITD leukemia cells at the time of graft injection. We observed a small but statistically significant reduction in photon flux at day 14 in the *Nlrp6*$^{-/-}$ T cell group, indicating enhanced early-phase tumor clearance (**Figure 7A, C**). However, there was no difference in tumor related mortality (TRM) *in vitro* cytotoxicity, *in vitro* degranulation, or production of cytotoxic molecules (**Figure 7B, D, supplemental Figure 8a-c**). These data indicated that Nlrp6 mildly restrains early donor T cell GVT likely via its effects on the early phase of T cell activation and proliferation. However, Nlrp6

had no effect of T cell cytotoxicity and, consistent with this, did not influence global GVT as measured by TRM.

NLRP6 expression is decreased in donor T cells from patients with aGVHD.

To test whether decrease Nlrp6 expression in donor T cells was associated with aGVHD in human allogeneic HSCT recipients, we measured its expression in donor T cells from patients with aGVHD relative to healthy controls. Patient characteristics are shown in supplemental Table1. Consistent with our murine data, Nlrp6 expression was significantly decreased in peripheral blood CD4+ and CD8+ T cells from patients with aGVHD (**Figure 8A-F, supplemental Figure 9a-f**). Thus, decreased donor T cell Nlrp6 expression is associated with aGVHD in both humans and mice.

DISCUSSION

We previously reported that Nlrp6 deficiency in host non-hematopoietic cells ameliorated aGVHD in an inflammasome- and gut microbiome- independent manner[10]. In addition to host tissue-dependent factors, donor T cell-dependent factors are also critical for acute GVHD pathogenesis. [2-4, 9, 12, 34-41]. Based on these observations, and prior to our work here, it was not known whether Nlrp6 in donor T cells regulated allo-immune responses. Therefore, we tested the role of Nlrp6 in donor T cells using multiple murine models of aGVHD. Based on Nlrp6's effect in host tissues[9], we hypothesized that Nlrp6 deficiency in donor T cells would reduce aGVHD. To our surprise, we found that *Nlrp6*$^{-/-}$ T cells aggravated aGVHD in MHC mismatched and haploidentical aGVHD models thereby uncovering a unique, suppressive role for Nlrp6 in allogeneic T cell responses.

Allogeneic HCT conditioning (e.g., total body irradiation and high dose chemotherapy) causes tissue damage leading to the release of PAMPs, such as lipopolysaccharide (LPS), and DAMPs, such as HMGB-1[42]. PAMPs and DAMPs activate host- and donor-derived antigen presenting cells (APCs)[43-45] , which subsequently stimulate donor allogeneic T cells. These stimulated donor T cells proliferate and migrate into target organs where they cause tissue damage resulting in clinical signs and symptoms of aGVHD[1]. DAMPs and PAMPs are recognized by the NLRP6 inflammasome, which then regulates inflammatory responses[3, 4]. In addition, DAMPs and PAMPs influence T cell activation and cytokine production[18, 46]. To determine whether conditioning-induced DAMPs and PAMPs contribute to the Nlrp6-dependent regulation of allogeneic T cells, we utilized the conditioning free B6 into B6D2F1 model.

Even in the absence of cytotoxic conditioning, aGVHD was worse in allogeneic recipients of *Nlrp6*$^{-/-}$ T cells. These data suggested that Nlrp6 negatively regulates allogeneic T cells independent of conditioning-related induction of DAMPs and PAMPs. However, we can't exclude the possibility that Nlrp6 in T cells may regulate these pathways directly.

Nlrp6 plays an important role in microbiome-dependent intestinal immune responses[3, 4]. However, Nlrp6 possesses both proinflammatory and anti-inflammatory abilities depending on cell and environmental context [9, 47]. To eliminate environment factors, we performed BMT experiments in Japan and the United States. We observed similarly worsened aGVHD with allogeneic *Nlrp6*$^{-/-}$ T cells at both institutions, suggesting that Nlrp6 is a cell-intrinsic regulator of allogeneic T cell.

Nlrp6 expression increased early after *in vitro* nonspecific TCR stimulation agreeing with a previous study showing that Nlrp6 expression increased upon Th1 differentiation[15, 48]. To determine the cell-intrinsic role of Nlrp6 in allo-stimulated T cells, we assessed proliferation and IFN-γ production *in vitro*, both of which were increased in *Nlrp6*$^{-/-}$ T cells. We also found that Tox expression early after allo-BMT (at day 7 and 14) in donor CD4+ and CD8+ T cells was higher in *Nlrp6*$^{-/-}$ T cells. These data suggested an intrinsic inhibitory role for Nlrp6 on allogeneic T cell proliferation and IFN-γ production.

Nlrp6 has inflammasome-dependent and -independent functions that can be either protective or deleterious and vary according to environmental context[2-4, 9, 12, 34-40]. As such, it is perhaps unsurprising that our data on proliferation and IFN-γ production in the context of alloimmunity are contrary to a prior study demonstrating that in the context of nonspecific polyclonal activation and an adoptive transfer model of colitis that *Nlrp6*$^{-/-}$ T cells proliferated to a similar extent, produced less IFN-γ, and had defective Th1 polarization[15]. The authors of the prior study concluded that Nlrp6$^{-/-}$ T cells produced lower levels of IFN-γ likely due to increased caspase-I activation and cell death, which are downstream of inflammasome activation. In our hands, *Nlrp6*$^{-/-}$ T cell proliferation was increased and unaffected by caspase 1 inhibition. The production of the inflammasome-activated cytokines, IL-1β and IL-18 was also unaffected by caspase 1 inhibition. However, we did observe increased apoptosis and exhaustion in Nlrp6 deficient allogeneic T cells on day 14 after allo-BMT. Therefore, the observed increase in proliferation of allogeneic Nlrp6$^{-/-}$ T cells may be a compensatory response to increased cell death, rather than reflecting isolated hyper activation. Collectively, the prior study and our data suggest that

Nlrp6 regulates T cell activation, IFN-γ production, apoptosis, and exhaustion in both an inflammasome-dependent and -independent manner depending on environmental context.

One potential contextual factor driving the discrepancies between our studied and Radulovic et al. may be due to pleiotropic effects on Nlrp6 on T cells receiving a nonspecific TCR stimulus (polyclonal activation) versus allogeneic stimuli used in our studies. Further studies will need to clarify the mechanisms underlying these potential pleiotropic effects, potentially by using Nlrp6$^{R39E\&W50E}$ mutant mice that enable the distinction between inflammasome-dependent and -independent functions of Nlrp6[41]. Despite Nlrp6's pleiotropic inflammasome-dependent and -independent effects, our *in vitro* results were consistent with our *in vivo* data where T cell accumulation, activation, and IFN-γ production were increased in allogeneic HCT recipients of *Nlrp6*$^{-/-}$ T cells. Our data are therefore the first to demonstrate allogeneic T cell-intrinsic regulation by Nlrp6. In addition, Nlrp6 expression was significantly decreased in peripheral blood CD4+ and CD8+ T cells from patients with aGVHD, which is consistent with our murine data. Collectively, these data suggested that decreased donor T cell Nlrp6 expression is associated with aGVHD.

MHC- matched hematopoietic stem grafts remain the most common donor type used clinically. To confirm that *Nlrp6*$^{-/-}$ donor T cells aggravated aGVHD in the absence of any MHC mismatch, we used the B6 into C3H.sw model[49, 50]. Unexpectedly, there was no difference in survival between WT and *Nlrp6*$^{-/-}$ T cell recipients. In comparison to our main MHC mismatched models, the B6 into C3H.sw model is primarily driven by CD8+ rather than CD4+ allogeneic T cells. To test whether the dominant CD8+ allogeneic T cell responses in the B6 into C3H.sw model were "masking" any CD4+ Nlrp6-specific effects, we performed transplants using purified CD4+ or CD8+ donor T cells. In both MHC matched and mismatched models, aGVHD was aggravated only by CD4+ but not CD8+ *Nlrp6*$^{-/-}$ donor T cells. Thus, Nlrp6 ameliorates allogeneic CD4+ T cell-mediated murine aGVHD. The mechanistic reason for Nlrp6's more prominent regulatory role in CD4+ T cells may relate to its greater effect of a Zap-70-Erk pathway downstream of the T cell receptor discussed below, which will require careful genetic confirmation in future *in vivo* studies.

Helper T cells differentiate into subsets including Th1, Th2, Th17, and Tregs. Of these subsets, Th1 and Th17 cells primarily aggravate aGVHD whereas Th2 and Treg mainly ameliorate aGVHD[1]. Because the

effect on Nlrp6 on murine aGVHD was primarily restricted to CD4+ cells, we determined whether Nlrp6 regulated CD4+ T cell differentiation. Consistent with our *in vivo* data, there was a trend towards increased Th1 *in vitro* polarization in *Nlrp6*$^{-/-}$ T cells whereas there was no effect on Th2 or Th17 polarization. We also tested whether Nlrp6 influenced regulatory T cell suppressive function *in vitro*, but we did not observe any difference between WT or *Nlrp6*$^{-/-}$ Tregs. Our data are consistent with another report showing no effect of Nlrp6 on Th2, Th17, or Treg differentiation[15]. However, we observed enhanced Th1 differentiation in Nlrp6 deficient T cells whereas another group reported the opposite effect[15]. As discussed above, careful examination of differences in experimental protocols between our studies will be required to determine the reason for this discrepancy. Nevertheless, our finding that Nlrp6 deficiency augments Th1 priming is consistent with our in vivo data showing enhanced production of the Th1 cytokine IFN-γ by *Nlrp6*$^{-/-}$ allogeneic T cells. Collectively, our data suggest that Nlrp6 may partially inhibit Th1 priming rather than polarization, which may lead to protection against acute GVHD.

Allogeneic T cell-mediated aGVHD and GVT responses are tightly linked, but CD8+ T cell cytolytic activity is critical for the GVT effect[1, 33]. Since Nlrp6 did not affect CD8+ T cell-mediated aGVHD-related mortality, we also tested if it affected GVT responses. Although CD8+ T cells from *Nlrp6*$^{-/-}$ mice showed greater activation than WT-T cells, surprisingly, tumor related mortality (TRM) and *in vitro* cytotoxic T cell killing were not altered. In addition, degranulation and cytotoxic protein production were not altered in CD8+ *Nlrp6*$^{-/-}$ T cells. However, a statistically significant reduction in photon flux was observed at day 14 in the Nlrp6$^{-/-}$ group compared with WT, indicating enhanced early tumor clearance. These findings are consistent with our *in vitro* and *in vivo* GVHD studies, in which *Nlrp6*$^{-/-}$ T cells demonstrated increased expansion and Erk phosphorylation during early T cell activation. However, this early advantage may later be counteracted by increased apoptosis and T cell exhaustion observed at later time points in allogenic *Nlrp6*$^{-/-}$ T cells in comparable over GVT measured by TRM at later stages following allo-BMT.

TCR signaling pathways are important for aGVHD pathogenesis and are targeted by many anti-aGVHD therapies[1]. With this in mind, we explored molecular mechanisms of Nlrp6-mediated regulation of CD4+ allogeneic T cells by determining whether Nlrp6 regulates their TCR signal transduction. We found that Nlrp6 negatively regulated a Zap-70/Erk pathway, but its absence did not globally alter TCR or cytokine receptor signaling because Lck and Stat3 activation were unaffected. Treatment with an Erk inhibitor had a greater and more consistent effect on Erk phosphorylation in both *Nlrp6*$^{-/-}$ and WT T

cells, albeit to a lesser extent in WT T cells. In addition, the inhibitor experiment demonstrates drug efficacy, not pathway mediation. These results are consistent with Zap-70 and Erk's ability to enhance Th1 priming and the importance of phosphorylated Erk for allogeneic T cell activation in aGVHD. However, precisely how Nlrp6 exclusively regulates Zap-70/Erk signaling more prominently in CD4+ T cells is still under investigation.

To confirm our murine findings in human, we measured Nlrp6 expression in T cells from patients with aGVHD versus healthy controls. Nlrp6 expression was significantly reduced in peripheral blood CD4+ and CD8+ T cells from patients with aGVHD. These results suggest that measuring and longitudinally monitoring *Nlrp6* expression in T cells may serve as a potential biomarker of donor T cell activation and predict GVHD onset or severity. However, further clinical studies with larger patient cohorts will be necessary to confirm this.

Chimeric antigen receptor (CAR) T cell therapy is increasingly being used for refractory and relapsed acute lymphoblastic leukemia, malignant lymphoma,[51] and multiple myeloma[52, 53]. Current CAR-T cell products are all manufactured from autologous T cells; however, it is often not feasible to generate autologous CAR-T cells, particularly from heavily pre-treated patients[54]. Third-party allogeneic CAR-T cells may offer an off-the-shelf solution but are limited by their risk for causing aGVHD[54]. Thus, augmenting Nlrp6 expression in allogenic CAR-T cells may be an opportunity to mitigate their GVHD potential.

There are several limitations of our study. First, Nlrp6 ligands are not yet defined thereby making it difficult to specifically modulate Nlrp6 function. Taurine may be an Nlrp6 activator in epithelial cells[37], and it enhances anti-tumor CD8+ T cell upon PD-1 blockade[55]. Nevertheless, it is not known if taurine directly regulates Nlrp6 in T cells. Second, it is not clear exactly why and how Nlrp6 regulates the Zap-70/Erk pathway only in CD4+ T cells. Third, while Nlrp6 expression was reduced in allogeneic T cells of patients with aGVHD, the functional impact of this reduced expression in clinical aGVHD is not yet established. Finally, it is possible that Nlrp6 has functions not identified here that are important for regulating allogeneic T cell function. Identifying these other functions may help avoid any unintended consequences of therapeutically targeting Nlrp6.

In conclusion, we uncovered a novel cell-intrinsic inhibitory function of Nlrp6 in CD4+ allogeneic T cells. Mechanistically, Nlrp6 limited CD4+ T cell activation, in part by inhibiting Zap-70-Erk1/2 signal transduction downstream of TCR activation, resulting in reduced GVHD and decreased inflammatory Th1 differentiation while maintaining robust GVT responses. Notably, the beneficial effects of Nlrp6 on donor T cells oppose its detrimental effects on intestinal epithelial cells during aGVHD indicating that Nlrp6 has antagonistic cell type- and context- specific functions in aGVHD. Therefore, ex vivo augmentation of Nlrp6 in donor T cells or selectively augmenting it in T cells in vivo might be useful for reducing aGVHD while preserving GVT.

REFERENCES

1. Zeiser R, Blazar BR. Acute Graft-versus-Host Disease - Biologic Process, Prevention, and Therapy. N Engl J Med. 2017;377(22):2167-2179.
2. Anand PK, Malireddi RK, Lukens JR, et al. NLRP6 negatively regulates innate immunity and host defence against bacterial pathogens. Nature. 2012;488(7411):389-393.
3. Elinav E, Strowig T, Kau AL, et al. NLRP6 inflammasome regulates colonic microbial ecology and risk for colitis. Cell. 2011;145(5):745-757.
4. Chen GY, Liu M, Wang F, Bertin J, Nunez G. A functional role for Nlrp6 in intestinal inflammation and tumorigenesis. J Immunol. 2011;186(12):7187-7194.
5. Sanches RCO, Souza C, Marinho FV, et al. NLRP6 Plays an Important Role in Early Hepatic Immunopathology Caused by Schistosoma mansoni Infection. Front Immunol. 2020;11:795.
6. Valino-Rivas L, Cuarental L, Nunez G, Sanz AB, Ortiz A, Sanchez-Nino MD. Loss of NLRP6 expression increases the severity of acute kidney injury. Nephrol Dial Transplant. 2020;35(4):587-598.
7. Ydens E, Demon D, Lornet G, et al. Nlrp6 promotes recovery after peripheral nerve injury independently of inflammasomes. J Neuroinflammation. 2015;12:143.
8. Schneider KM, Mohs A, Gui W, et al. Imbalanced gut microbiota fuels hepatocellular carcinoma development by shaping the hepatic inflammatory microenvironment. Nat Commun. 2022;13(1):3964.
9. Venuprasad K, Theiss AL. NLRP6 in host defense and intestinal inflammation. Cell Rep. 2021;35(4):109043.
10. Toubai T, Fujiwara H, Rossi C, et al. Host NLRP6 exacerbates graft-versus-host disease independent of gut microbial composition. Nat Microbiol. 2019;4(5):800-812.
11. Seregin SS, Golovchenko N, Schaf B, Chen J, Eaton KA, Chen GY. NLRP6 function in inflammatory monocytes reduces susceptibility to chemically induced intestinal injury. Mucosal Immunol. 2017;10(2):434-445.
12. Cai S, Paudel S, Jin L, et al. NLRP6 modulates neutrophil homeostasis in bacterial pneumonia-derived sepsis. Mucosal Immunol. 2021;14(3):574-584.
13. Chang L, Xu L, Tian Y, et al. NLRP6 deficiency suppresses colorectal cancer liver metastasis growth by modulating M-MDSC-induced immunosuppressive microenvironment. Biochim Biophys Acta Mol Basis Dis. 2024;1870(3):167035.
14. Tao Q, Xu D, Jia K, et al. NLRP6 Serves as a Negative Regulator of Neutrophil Recruitment and Function During Streptococcus pneumoniae Infection. Front Microbiol. 2022;13:898559.
15. Radulovic K, Ayata CK, Mak'Anyengo R, et al. NLRP6 Deficiency in CD4 T Cells Decreases T Cell Survival Associated with Increased Cell Death. J Immunol. 2019;203(2):544-556.
16. Reddy P, Maeda Y, Liu C, Krijanovski OI, Korngold R, Ferrara JL. A crucial role for antigen-presenting cells and alloantigen expression in graft-versus-leukemia responses. Nat Med. 2005;11(11):1244-1249.
17. Reddy P, Sun Y, Toubai T, et al. Histone deacetylase inhibition modulates indoleamine 2,3-dioxygenase-dependent DC functions and regulates experimental graft-versus-host disease in mice. J Clin Invest. 2008;118(7):2562-2573.
18. Toubai T, Rossi C, Oravecz-Wilson K, et al. Siglec-G represses DAMP-mediated effects on T cells. JCI Insight. 2017;2(14):e92293.
19. Hill GR, Cooke KR, Teshima T, et al. Interleukin-11 promotes T cell polarization and prevents acute graft-versus-host disease after allogeneic bone marrow transplantation. J Clin Invest. 1998;102(1):115-123.
20. Toubai T, Sun Y, Tawara I, et al. Ikaros-Notch axis in host hematopoietic cells regulates experimental graft-versus-host disease. Blood. 2011;118(1):192-204.
21. Toubai T, Tawara I, Sun Y, et al. Induction of acute GVHD by sex-mismatched H-Y antigens in the absence of functional radiosensitive host hematopoietic-derived antigen-presenting cells. Blood. 2012;119(16):3844-3853.

22. Mathewson ND, Jenq R, Mathew AV, et al. Gut microbiome-derived metabolites modulate intestinal epithelial cell damage and mitigate graft-versus-host disease. Nat Immunol. 2016;17(5):505-513.
23. Reddy P, Negrin R, Hill GR. Mouse models of bone marrow transplantation. Biol Blood Marrow Transplant. 2008;14(1 Suppl 1):129-135.
24. Au-Yeung BB, Levin SE, Zhang C, et al. A genetically selective inhibitor demonstrates a function for the kinase Zap70 in regulatory T cells independent of its catalytic activity. Nat Immunol. 2010;11(12):1085-1092.
25. Jirmanova L, Giardino Torchia ML, Sarma ND, Mittelstadt PR, Ashwell JD. Lack of the T cell-specific alternative p38 activation pathway reduces autoimmunity and inflammation. Blood. 2011;118(12):3280-3289.
26. Au-Yeung BB, Shah NH, Shen L, Weiss A. ZAP-70 in Signaling, Biology, and Disease. Annu Rev Immunol. 2018;36:127-156.
27. Chang CF, D'Souza WN, Ch'en IL, Pages G, Pouyssegur J, Hedrick SM. Polar opposites: Erk direction of CD4 T cell subsets. J Immunol. 2012;189(2):721-731.
28. D'Souza WN, Chang CF, Fischer AM, Li M, Hedrick SM. The Erk2 MAPK regulates CD8 T cell proliferation and survival. J Immunol. 2008;181(11):7617-7629.
29. Griffith CE, Zhang W, Wange RL. ZAP-70-dependent and -independent activation of Erk in Jurkat T cells. Differences in signaling induced by H2o2 and Cd3 cross-linking. J Biol Chem. 1998;273(17):10771-10776.
30. Lu WL, Zhang L, Song DZ, et al. NLRP6 suppresses the inflammatory response of human periodontal ligament cells by inhibiting NF-kappaB and ERK signal pathways. Int Endod J. 2019;52(7):999-1009.
31. Xu D, Wu X, Peng L, et al. The Critical Role of NLRP6 Inflammasome in Streptococcus pneumoniae Infection In Vitro and In Vivo. Int J Mol Sci. 2021;22(8):3876.
32. Lu SX, Alpdogan O, Lin J, et al. STAT-3 and ERK 1/2 phosphorylation are critical for T-cell alloactivation and graft-versus-host disease. Blood. 2008;112(13):5254-5258.
33. Bleakley M, Riddell SR. Molecules and mechanisms of the graft-versus-leukaemia effect. Nat Rev Cancer. 2004;4(5):371-380.
34. Hara H, Seregin SS, Yang D, et al. The NLRP6 Inflammasome Recognizes Lipoteichoic Acid and Regulates Gram-Positive Pathogen Infection. Cell. 2018;175(6):1651-1664.e14.
35. Ghimire L, Paudel S, Jin L, Baral P, Cai S, Jeyaseelan S. NLRP6 negatively regulates pulmonary host defense in Gram-positive bacterial infection through modulating neutrophil recruitment and function. PLoS Pathog. 2018;14(9):e1007308.
36. Normand S, Delanoye-Crespin A, Bressenot A, et al. Nod-like receptor pyrin domain-containing protein 6 (NLRP6) controls epithelial self-renewal and colorectal carcinogenesis upon injury. Proc Natl Acad Sci U S A. 2011;108(23):9601-9606.
37. Levy M, Thaiss CA, Zeevi D, et al. Microbiota-Modulated Metabolites Shape the Intestinal Microenvironment by Regulating NLRP6 Inflammasome Signaling. Cell. 2015;163(6):1428-1443.
38. Wlodarska M, Thaiss CA, Nowarski R, et al. NLRP6 inflammasome orchestrates the colonic host-microbial interface by regulating goblet cell mucus secretion. Cell. 2014;156(5):1045-1059.
39. Volk JK, Nystrom EEL, van der Post S, et al. The Nlrp6 inflammasome is not required for baseline colonic inner mucus layer formation or function. J Exp Med. 2019;216(11):2602-2618.
40. Wang P, Zhu S, Yang L, et al. Nlrp6 regulates intestinal antiviral innate immunity. Science. 2015;350(6262):826-830.
41. Li R, Zan Y, Wang D, et al. A mouse model to distinguish NLRP6-mediated inflammasome-dependent and -independent functions. Proc Natl Acad Sci U S A. 2024;121(6):e2321419121.
42. Toubai T, Mathewson ND, Magenau J, Reddy P. Danger Signals and Graft-versus-host Disease: Current Understanding and Future Perspectives. Front Immunol. 2016;7:539.
43. Toubai T, Hou G, Mathewson N, et al. Siglec-G-CD24 axis controls the severity of graft-versus-host disease in mice. Blood. 2014;123(22):3512-3523.

44. Cooke KR, Hill GR, Crawford JM, et al. Tumor necrosis factor- alpha production to lipopolysaccharide stimulation by donor cells predicts the severity of experimental acute graft-versus-host disease. J Clin Invest. 1998;102(10):1882-1891.
45. Brennan TV, Lin L, Huang X, et al. Heparan sulfate, an endogenous TLR4 agonist, promotes acute GVHD after allogeneic stem cell transplantation. Blood. 2012;120(14):2899-2908.
46. Mills KH. TLR-dependent T cell activation in autoimmunity. Nat Rev Immunol. 2011;11(12):807-822.
47. Angosto-Bazarra D, Molina-Lopez C, Pelegrin P. Physiological and pathophysiological functions of NLRP6: pro- and anti-inflammatory roles. Commun Biol. 2022;5(1):524.
48. Chenuet P, Marquant Q, Fauconnier L, et al. NLRP6 negatively regulates type 2 immune responses in mice. Allergy. 2022;77(11):3320-3336.
49. Baker MB, Riley RL, Podack ER, Levy RB. Graft-versus-host-disease-associated lymphoid hypoplasia and B cell dysfunction is dependent upon donor T cell-mediated Fas-ligand function, but not perforin function. Proc Natl Acad Sci U S A. 1997;94(4):1366-1371.
50. Marks L, Altman NH, Podack ER, Levy RB. Donor T cells lacking Fas ligand and perforin retain the capacity to induce severe GvHD in minor histocompatibility antigen mismatched bone-marrow transplantation recipients. Transplantation. 2004;77(6):804-812.
51. Kochenderfer JN, Dudley ME, Kassim SH, et al. Chemotherapy-refractory diffuse large B-cell lymphoma and indolent B-cell malignancies can be effectively treated with autologous T cells expressing an anti-CD19 chimeric antigen receptor. J Clin Oncol. 2015;33(6):540-549.
52. Grupp SA, Kalos M, Barrett D, et al. Chimeric antigen receptor-modified T cells for acute lymphoid leukemia. N Engl J Med. 2013;368(16):1509-1518.
53. Garfall AL, Maus MV, Hwang WT, et al. Chimeric Antigen Receptor T Cells against CD19 for Multiple Myeloma. N Engl J Med. 2015;373(11):1040-1047.
54. Aparicio C, Acebal C, Gonzalez-Vallinas M. Current approaches to develop "off-the-shelf" chimeric antigen receptor (CAR)-T cells for cancer treatment: a systematic review. Exp Hematol Oncol. 2023;12(1):73.
55. Ping Y, Shan J, Liu Y, et al. Taurine enhances the antitumor efficacy of PD-1 antibody by boosting CD8(+) T cell function. Cancer Immunol Immunother. 2023;72(4):1015-1027.

Figure legends

Figure 1. *Nlrp6*$^{-/-}$ donor T cells exacerbate acute GVHD in MHC mismatched and haploidentical BMT models.

A-B, BALB/c recipients received 7 Gy (**A**) or 8.5 Gy (**B**) total body irradiation (TBI) on day −1 and were transplanted with 1×10^6 CD90.2+ syngeneic BALB/c or allogeneic major histocompatibility (MHC)-mismatched B6 WT or *Nlrp6*$^{-/-}$ splenic T cells along with 5×10^6 WT syngeneic or allogeneic T cell-depleted bone marrow (TCD-BM) cells. n=4-24 per group. Data are pooled from 2-3 experiments. **C-D,** B6D2F1 recipients received 11 Gy TBI on day −1 and were transplanted with 3.5×10^6 CD90.2+ syngeneic B6D2F1 or allogeneic MHC-haplotype mismatched B6 WT or *Nlrp6*$^{-/-}$ splenic T cells along with 5×10^6 WT syngeneic or allogeneic TCD-BM cells. n=7-17 per group. Data are pooled from 3 experiments. Survivals is shown in each panel. BMTs were performed in Yamagata, Japan (**A, C**) or Michigan, USA (**B, D**). **E,** Representative histopathological images of the small bowel (top panels) and large bowel (bottom panels) 14 days after BMT in the model described in Figure 1 A are shown on the left side of panel E. Histopathological GVHD scores for the small and large bowel are shown on the right side of panel E (n=22-30 per group). Data are pooled from 7 experiments. **F,** Overall survival is shown of non-irradiated B6D2F1 animals that received 50×10^6 splenocytes from either syngeneic B6D2F1 or allogeneic MHC-haploidentical B6 WT *Nlrp6*$^{-/-}$ donors. n=3-11 per group. Data are pooled from 3 independent experiments. Statistical significance was analyzed using the Log-rank test (**A-D, F**) and a two-tailed Mann-Whitney U-test (**E**). * p<0.05, ** p<0.01.

Figure 2. Expansion, activation, and IFN-γ production are increased in *Nlrp6*$^{-/-}$ donor T cells following MHC-mismatched BMT.

A-F, BALB/c animals received 7 Gy TBI on day −1 and were transplanted with 0.5×10^6 CD90.2+ splenic T cells along with 5×10^6 TCD-BM cells from allogeneic MHC-mismatched B6 WT or *Nlrp6*$^{-/-}$ donors. Donor T cells in the spleen of recipient mice were analyzed on day 7 or day 14 after BMT. The numbers of allogeneic donor T cells (H-2K^b+) are shown in **A**. **(B)** The number of donor CD4+ (left panels) and CD8+ (right panels) T cells expressing Tox are shown. **(C)** The number of donor CD4+ (left panels) and CD8+ (right panels) T cells expressing IFN-γ are shown. **(D)** The number of donor CD4+ (left panels) and CD8+ (right panels) T cells expressing IFN-γ and TOX are shown. **(E)** The number of donor CD4+ (left panels) and CD8+ (right panels) early apoptotic T cells are shown. **(F)** The number of

whole T cells (left panel), CD4+ T cells (center panel), and CD8+ T cells (right panel) in the liver are shown. N=4-10 per group. Data are pooled from 2-3 independent experiments (**A-F**). Statistical significance was analyzed using a two-tailed Mann-Whitney U-test (**A-F**). *p<0.05, ** p<0.01. Data are shown as the mean ± SEM. All sample numbers are shown in the figure.

Figure 3. Proliferation, IFN-γ secretion, and DNA synthesis are increased in allogeneic and nonspecific TCR-stimulated *Nlrp6*$^{-/-}$ T cells.

A, C-D, An *in vitro*, mixed lymphocyte reaction (MLR) was performed using splenic CD90.2+ T cells from either B6 WT or *Nlrp6*$^{-/-}$ mice that were co-cultured for 96 or 120 hours with BMDCs (**A and C**) or splenocytes (**D**) derived from allogeneic BALB/c mice. Proliferating T cells were measured by ^{3}H-thymidine incorporation (CPM, count per minutes) during the last 16 hours of incubation (n=4) (**A**). IFN-γ secretion from T cells was measured by ELISA (n=4) (**C)**. T cells were labeled with CFSE and analyzed by flow cytometry (n=3-5) (**D**). **B, E,** Proliferation of *in vitro*, non-specific TCR stimulated (anti-CD3/28 antibodies) B6 WT and *Nlrp6*$^{-/-}$ T cells was measured following ^{3}H-thymidine incorporation during the last 16 h of incubation (n=4) (**B**) or flow cytometric analysis of BrdU incorporation in CD4+ or CD8+ T cells at 72 hours after stimulation (**E**) (n=5). Statistical significance was determined using a two-tailed Mann-Whitney U-test (**A-E**). *p<0.05, **p<0.01, ***p<0.001. Data are shown as the mean ± SEM.

Figure 4. NLRP6 regulates allogeneic CD4+ T cell mediated murine acute GVHD.

A, C3H.sw mice received 10.5 Gy TBI on day −1 and were transplanted with 1×10^{6} CD90.2+ syngeneic C3H.sw or allogeneic minor histocompatibility antigens (miHAs)-mismatched B6 WT or *Nlrp6*$^{-/-}$ splenic T cells along with either 5×10^{6} WT syngeneic or allogenic TCD-BM cells. n=6-10 per group. Data are pooled from 2 independent experiments. **B-C,** C3H.sw animals received 10.5 Gy TBI on day −1 and were transplanted with 0.5×10^{6} CD4+ (**B**) or CD8+ (**C**) splenic T cells from either miHAs-mismatched B6 WT or *Nlrp6*$^{-/-}$ donors along with 5×10^{6} TCD-BM cells from B6 WT mice. n=9-20 per group. Data are pooled from 2-4 independent experiments. **D-E,** BALB/c animals received 7 Gy TBI on day −1 and were transplanted with 0.5×10^{6} CD4+ (**D**) or CD8+ (**E**) splenic T cells from either MHC-mismatched B6 WT or *Nlrp6*$^{-/-}$ donors along with 5×10^{6} TCD-BM cells from B6-WT mice. n=10 per group. Data are pooled from 2 independent experiments. Survival is shown in each panel. Statistical significance was analyzed using a Log-rank test (**A-E**). *p<0.05, **p<0.01.

Figure 5. Th1 *in vitro* differentiation was enhanced in *Nlrp6*$^{-/-}$ CD4+ T cells.

A-C, CD4+ T cells from either B6 WT or *Nlrp6*$^{-/-}$ animals were cultured under Th1, Th2, or Th17 polarizing conditions for 5 or 6 days. Th1 differentiation indicated by the percentage of T-bet+ (left) or IFN-γ+ (right) cells is shown (n=5) (**A**). Th2 differentiation indicated by the percentage of GATA-3+ (left) or IL-4+ (right) cells is shown (n=3-4) (**B**). Th17 differentiation indicated by the percentage of RORγt+ (left) or IL-17A+ (right) cells is shown (n=6) (**C**). Statistical significance was determined using a two-tailed Mann-Whitney U-test (**A-C**). **p*<0.05. Data are shown as the mean ± SEM. **D,** A Treg suppression assay was performed using BMDCs from BALB/c mice as stimulators that were co-cultured with effector T cells (CD4+CD25-) and Tregs (CD4+CD25+) from either B6 WT or *Nlrp6*$^{-/-}$ mice at different ratios. T cell proliferation was measured following ^{3}H-thymidine incorporation during the last 16 hours of incubation. Data are representative of 4 independent experiments.

Figure 6. Zap-70 and Erk activation are enhanced in *Nlrp6*$^{-/-}$ CD4+ T cells.

A-B, T cells from either B6 WT or *Nlrp6*$^{-/-}$ mice were stimulated with anti-CD3/28 antibodies for 2-5 minutes. Phosphorylated Erk1/2 was then measured by flow cytometry (n=4). (**A**) Representative histograms of unstimulated (grey) and 2 minutes after stimulation (blue or red) are shown. (**B**) Percentage of pErk1/2+ cells in CD4+ (left) or CD8+ (right) cells are shown (n=6). Statistical significance was determined using a two-tailed Mann-Whitney U-test. **p*<0.05, ***p*<0.01. Data are shown as the mean ± SEM. **C,** T cells from either B6 WT or *Nlrp6*$^{-/-}$ mice were stimulated with anti-CD3/28 antibodies for 2 minutes in the presence of an Erk kinase inhibitor (FR180204, 20 μM). Phosphorylated Erk1/2 was then measured by flow cytometry. Representative histograms of control (grey) and 2 minutes after stimulation (blue or red) are shown (left panel). Percentage of pErk1/2+ cells in CD4+ or CD8+ cells are shown (n=4, right panel). Statistical significance was determined using a two-tailed Mann-Whitney U-test (**C**). **p*<0.05. Data are shown as the mean ± SEM.

Figure 7. GVT responses of *Nlrp6*$^{-/-}$ and WT T cells to Baf/3-ITD leukemia cells were equivalent.

A-C, BALB/c recipients received 7 Gy TBI on day -1 and were transplanted with 0.5×10^{6} CD90.2+ splenic T cells from either syngeneic BALB/c or allogeneic MHC-mismatched B6 WT or *Nlrp6*$^{-/-}$ donors along with 5×10^{6} WT syngeneic or allogeneic TCD-BM cells. Five hundred syngeneic Baf/3-ITD leukemia cells were co-infused with the graft. Leukemia cell growth was monitored using an In Vivo Imaging Systems (IVIS) on day 14 or 21 after allo BMT. Representative data from 1 of 3 experiments

are shown in **A**. Leukemia-related mortality is shown in **B**. Total ROI (photons/second) signal on post-transplantation day 14 or 21 is shown in **C**. n=8-9 per group. Data are pooled from 3 independent experiments. **D,** A CTL assay was performed using bulk MLR-activated T cells from B6 WT or *Nlrp6*$^{-/-}$ mice co-cultured with Baf/3-ITD leukemia cells at a ratio of 1:10-1:40 for 4 hours. The percentage of Annexin V+ leukemia cells was measured by flow cytometry and is depicted in **D** (n=3). Statistical significance was analyzed using a Log-rank test for panel **B** and a two-tailed Mann-Whitney U-test for panel **C**. The functions of WT B6 versus *Nlrp6*$^{-/-}$ T cells were analyzed with the two-tailed Mann-Whitney U-test (**D**). **p*<0.05, ***p*<0.01, ****p*<0.001. Data are shown as the mean ± SEM.

Figure 8. NLRP6 expression is reduced in T cells of aGVHD patients.

PBMCs of healthy donors (n=13) and aGVHD patients (n=8) were analyzed by spectral flow. MFI of NLRP6 was evaluated on multiple T cell subsets. Normality was assessed using the Shapiro-Wilk test. Statistical significance was analyzed using a two-tailed unpaired T-test (**A-B, D-F**) or two-tailed unpaired T-test with Welch correction (**C**). **p*<0.05. Data are shown as the mean ± SEM. All sample numbers are shown in the figure.

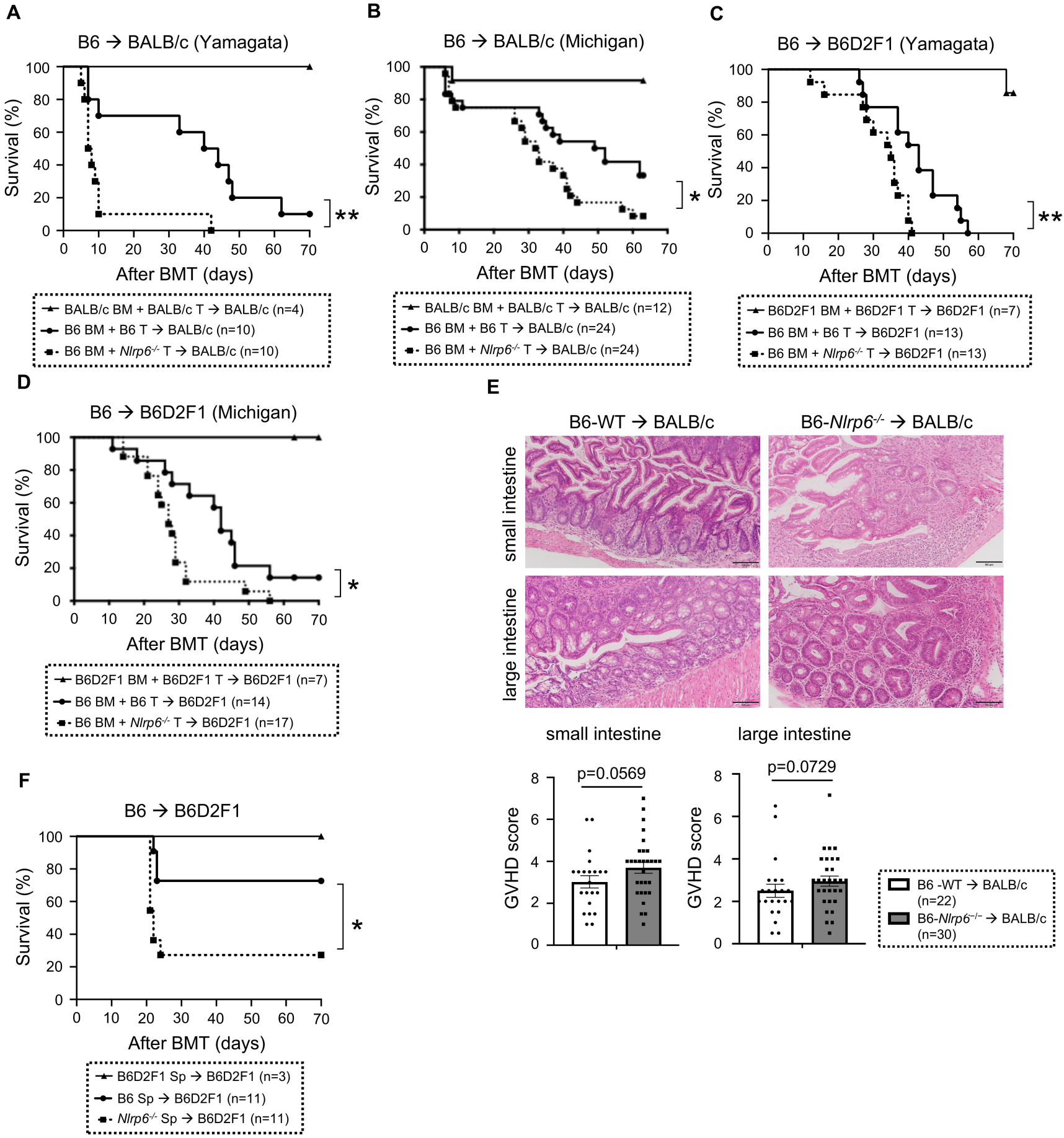
A
B6 → BALB/c (Yamagata)
Survival (%)
After BMT (days)
**
BALB/c BM + BALB/c T → BALB/c (n=4)
B6 BM + B6 T → BALB/c (n=10)
B6 BM + Nlrp6-/- T → BALB/c (n=10)
B
B6 → BALB/c (Michigan)
Survival (%)
After BMT (days)
*
BALB/c BM + BALB/c T → BALB/c (n=12)
B6 BM + B6 T → BALB/c (n=24)
B6 BM + Nlrp6-/- T → BALB/c (n=24)
C
B6 → B6D2F1 (Yamagata)
Survival (%)
After BMT (days)
**
B6D2F1 BM + B6D2F1 T → B6D2F1 (n=7)
B6 BM + B6 T → B6D2F1 (n=13)
B6 BM + Nlrp6-/- T → B6D2F1 (n=13)
D
B6 → B6D2F1 (Michigan)
Survival (%)
After BMT (days)
*
B6D2F1 BM + B6D2F1 T → B6D2F1 (n=7)
B6 BM + B6 T → B6D2F1 (n=14)
B6 BM + Nlrp6-/- T → B6D2F1 (n=17)
E
B6-WT → BALB/c
B6-Nlrp6-/- → BALB/c
small intestine
large intestine
small intestine
large intestine
p=0.0569
p=0.0729
GVHD score
GVHD score
B6 -WT → BALB/c (n=22)
B6-Nlrp6-/- → BALB/c (n=30)
F
B6 → B6D2F1
Survival (%)
After BMT (days)
*
B6D2F1 Sp → B6D2F1 (n=3)
B6 Sp → B6D2F1 (n=11)
Nlrp6-/- Sp → B6D2F1 (n=11)

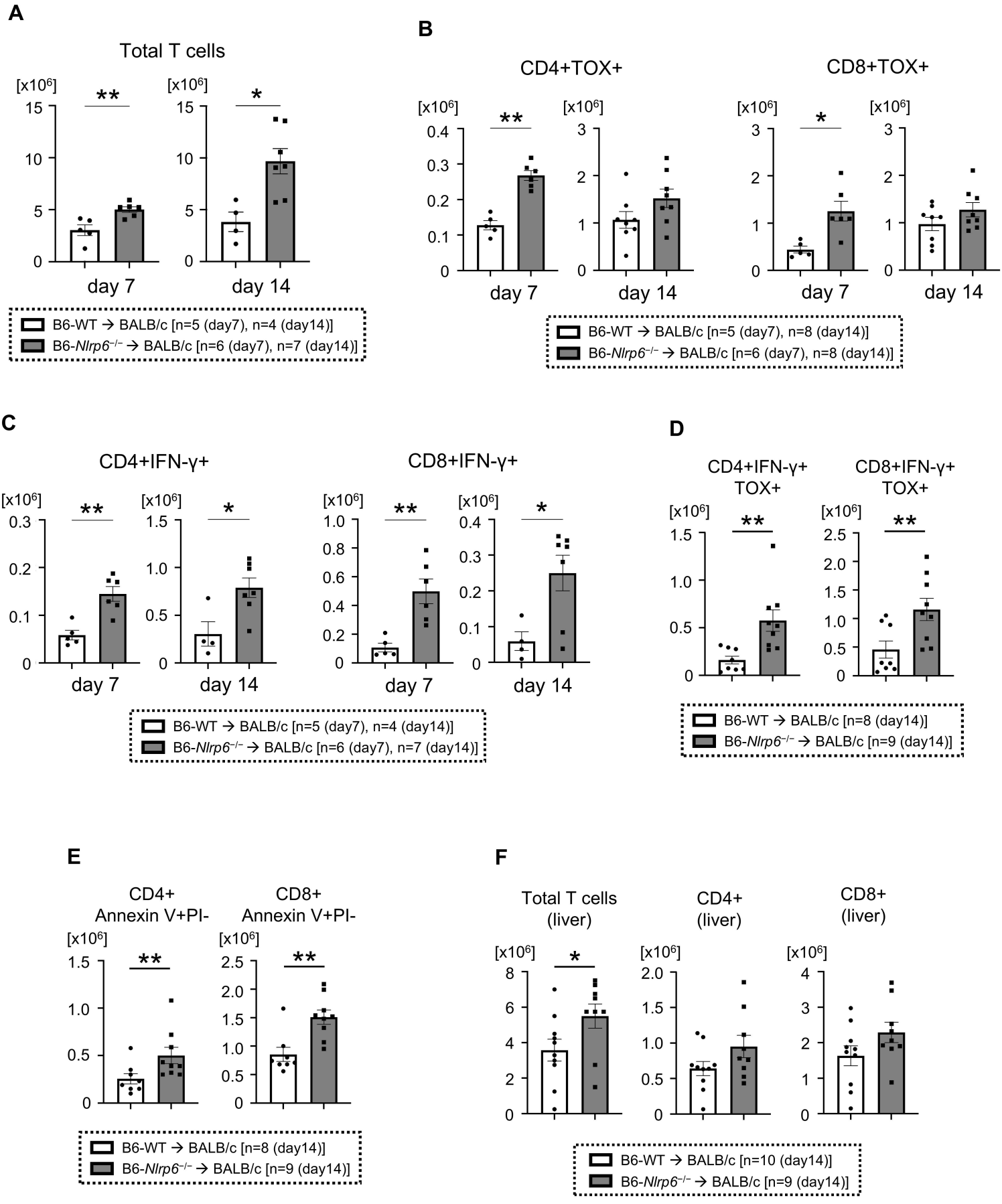
A
Total T cells
[x10⁶]
**
*
day 7
day 14
B6-WT → BALB/c [n=5 (day7), n=4 (day14)]
B6-Nlrp6⁻/⁻ → BALB/c [n=6 (day7), n=7 (day14)]
B
CD4+TOX+
CD8+TOX+
B6-WT → BALB/c [n=5 (day7), n=8 (day14)]
B6-Nlrp6⁻/⁻ → BALB/c [n=6 (day7), n=8 (day14)]
C
CD4+IFN-γ+
CD8+IFN-γ+
B6-WT → BALB/c [n=5 (day7), n=4 (day14)]
B6-Nlrp6⁻/⁻ → BALB/c [n=6 (day7), n=7 (day14)]
D
CD4+IFN-γ+ TOX+
CD8+IFN-γ+ TOX+
B6-WT → BALB/c [n=8 (day14)]
B6-Nlrp6⁻/⁻ → BALB/c [n=9 (day14)]
E
CD4+ Annexin V+PI-
CD8+ Annexin V+PI-
B6-WT → BALB/c [n=8 (day14)]
B6-Nlrp6⁻/⁻ → BALB/c [n=9 (day14)]
F
Total T cells (liver)
CD4+ (liver)
CD8+ (liver)
B6-WT → BALB/c [n=10 (day14)]
B6-Nlrp6⁻/⁻ → BALB/c [n=9 (day14)]

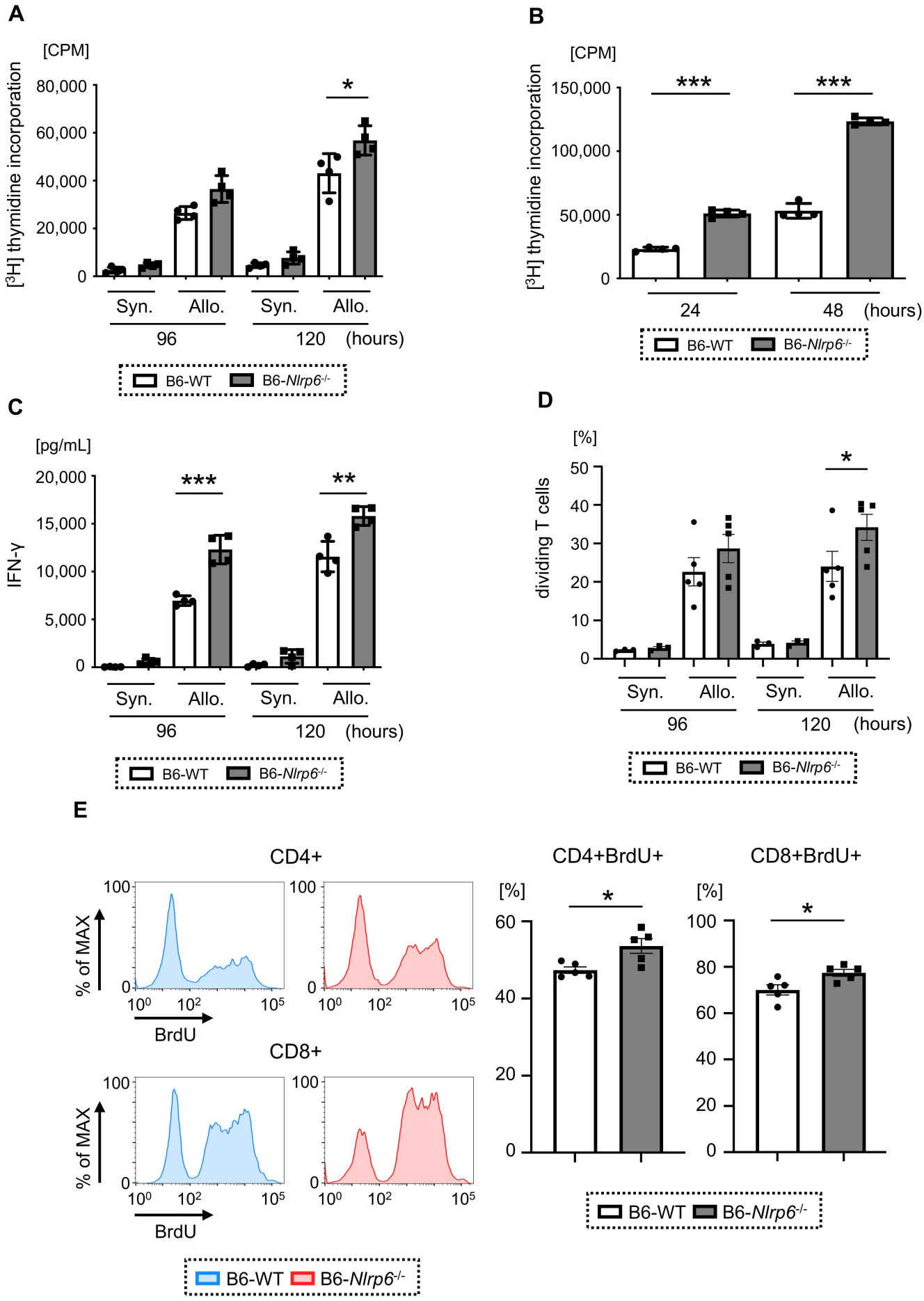
A
[CPM]
[3H] thymidine incorporation
80,000
60,000
40,000
20,000
0
*
Syn.
Allo.
Syn.
Allo.
96
120
(hours)
B6-WT
B6-Nlrp6-/-
B
[CPM]
[3H] thymidine incorporation
150,000
100,000
50,000
0
***
***
24
48
(hours)
B6-WT
B6-Nlrp6-/-
C
[pg/mL]
IFN-γ
20,000
15,000
10,000
5,000
0
***
**
Syn.
Allo.
Syn.
Allo.
96
120
(hours)
B6-WT
B6-Nlrp6-/-
D
[%]
dividing T cells
50
40
30
20
10
0
*
Syn.
Allo.
Syn.
Allo.
96
120
(hours)
B6-WT
B6-Nlrp6-/-
E
CD4+
CD8+
% of MAX
100
0
10^0
10^2
10^5
BrdU
B6-WT
B6-Nlrp6-/-
CD4+BrdU+
CD8+BrdU+
[%]
60
40
20
0
100
80
60
40
20
0
*
*
B6-WT
B6-Nlrp6-/-

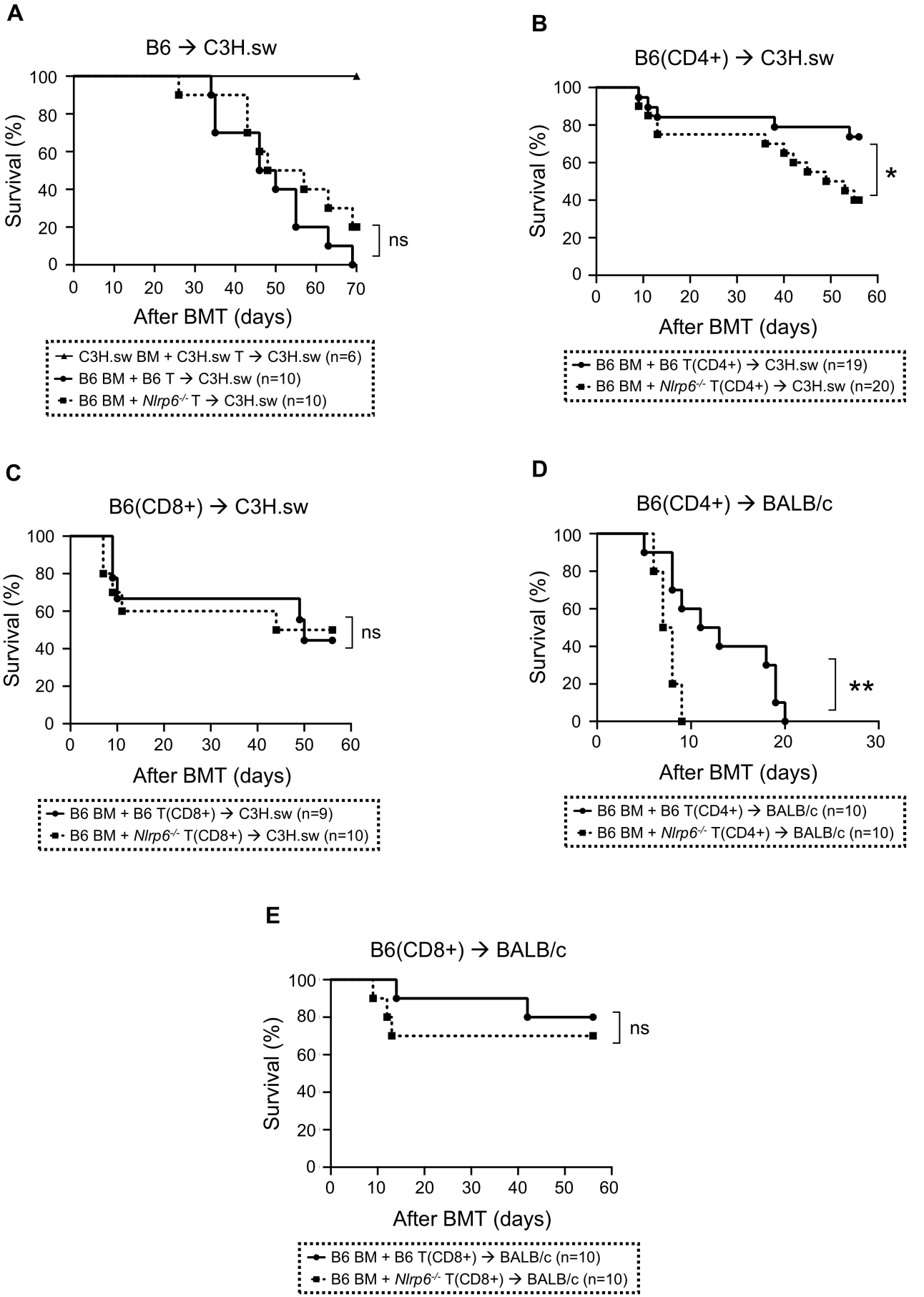
A
B6 → C3H.sw
Survival (%)
After BMT (days)
ns
C3H.sw BM + C3H.sw T → C3H.sw (n=6)
B6 BM + B6 T → C3H.sw (n=10)
B6 BM + Nlrp6-/- T → C3H.sw (n=10)
B
B6(CD4+) → C3H.sw
Survival (%)
After BMT (days)
*
B6 BM + B6 T(CD4+) → C3H.sw (n=19)
B6 BM + Nlrp6-/- T(CD4+) → C3H.sw (n=20)
C
B6(CD8+) → C3H.sw
Survival (%)
After BMT (days)
ns
B6 BM + B6 T(CD8+) → C3H.sw (n=9)
B6 BM + Nlrp6-/- T(CD8+) → C3H.sw (n=10)
D
B6(CD4+) → BALB/c
Survival (%)
After BMT (days)
**
B6 BM + B6 T(CD4+) → BALB/c (n=10)
B6 BM + Nlrp6-/- T(CD4+) → BALB/c (n=10)
E
B6(CD8+) → BALB/c
Survival (%)
After BMT (days)
ns
B6 BM + B6 T(CD8+) → BALB/c (n=10)
B6 BM + Nlrp6-/- T(CD8+) → BALB/c (n=10)

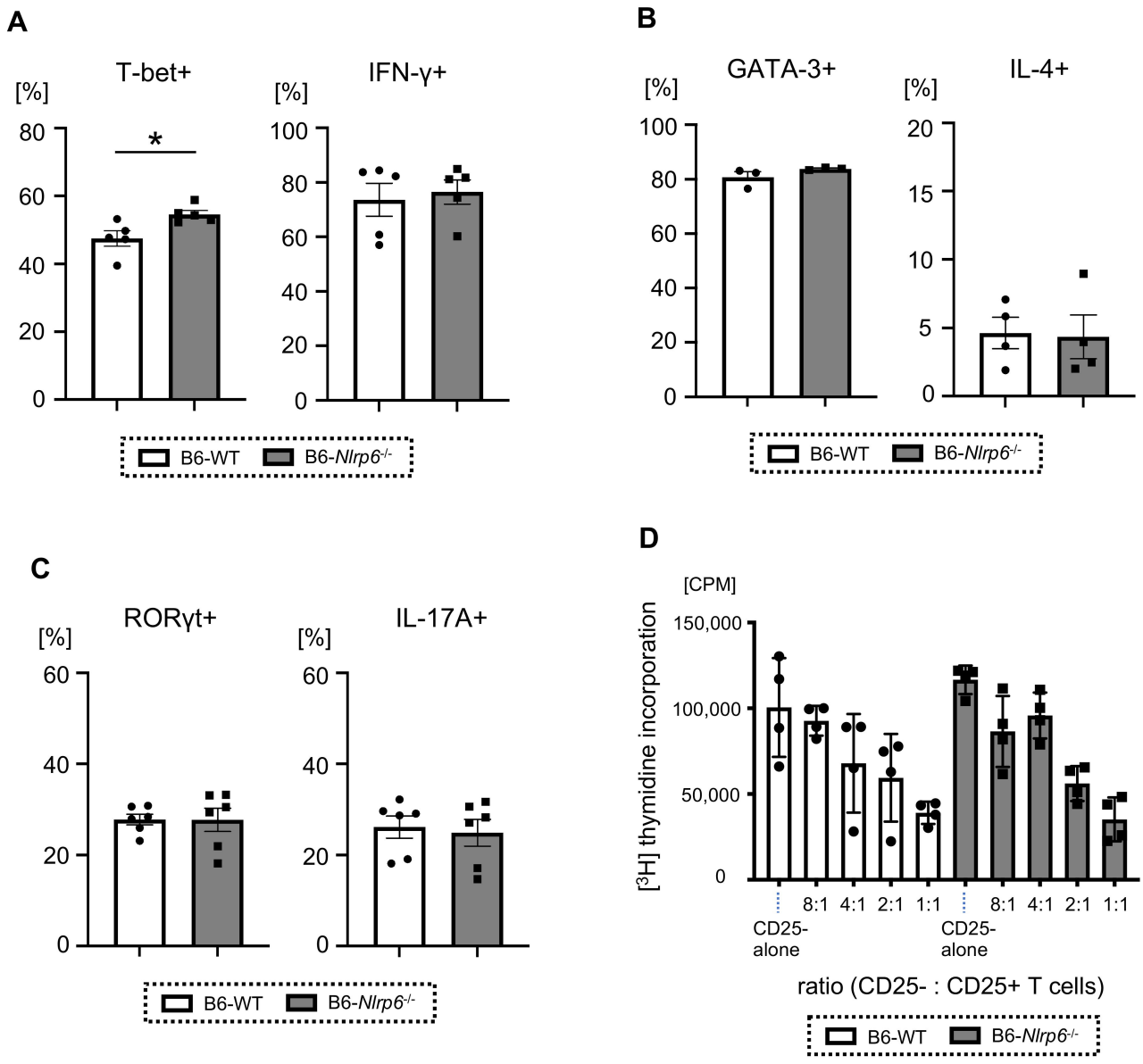
A
T-bet+
[%]
80
60
40
20
0
*
IFN-γ+
[%]
100
80
60
40
20
0
B6-WT
B6-Nlrp6-/-
B
GATA-3+
[%]
100
80
60
40
20
0
IL-4+
[%]
20
15
10
5
0
B6-WT
B6-Nlrp6-/-
C
RORγt+
[%]
60
40
20
0
IL-17A+
[%]
60
40
20
0
B6-WT
B6-Nlrp6-/-
D
[CPM]
[3H] thymidine incorporation
150,000
100,000
50,000
0
8:1
4:1
2:1
1:1
CD25-
alone
8:1
4:1
2:1
1:1
CD25-
alone
ratio (CD25- : CD25+ T cells)
B6-WT
B6-Nlrp6-/-

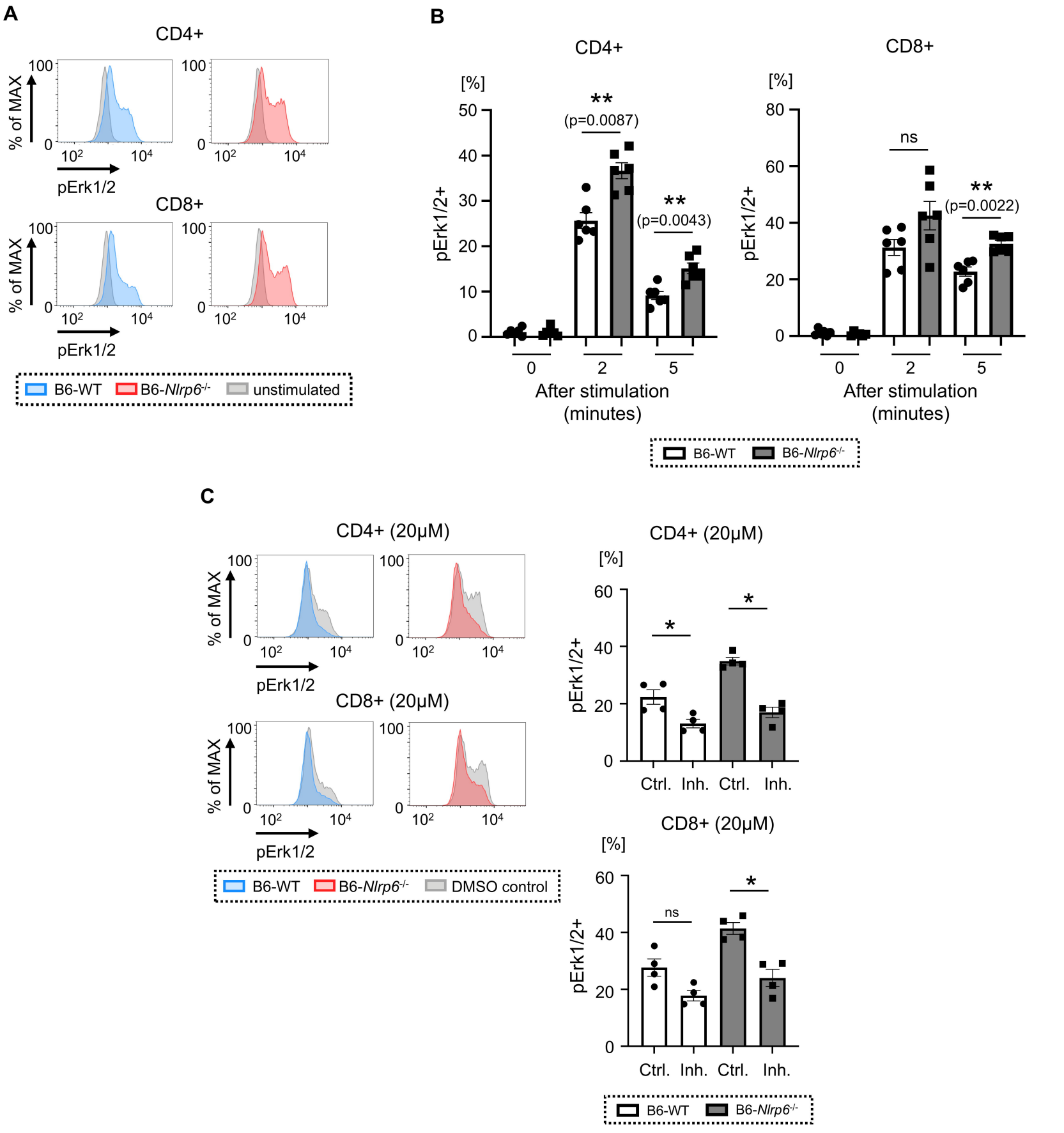
A
CD4+
% of MAX
100
0
10^2
10^4
pErk1/2
CD8+
B6-WT
B6-Nlrp6-/-
unstimulated
B
CD4+
CD8+
[%]
pErk1/2+
**
(p=0.0087)
**
(p=0.0043)
ns
**
(p=0.0022)
0
2
5
After stimulation
(minutes)
B6-WT
B6-Nlrp6-/-
C
CD4+ (20μM)
CD8+ (20μM)
% of MAX
pErk1/2
B6-WT
B6-Nlrp6-/-
DMSO control
*
ns
Ctrl.
Inh.
Ctrl.
Inh.

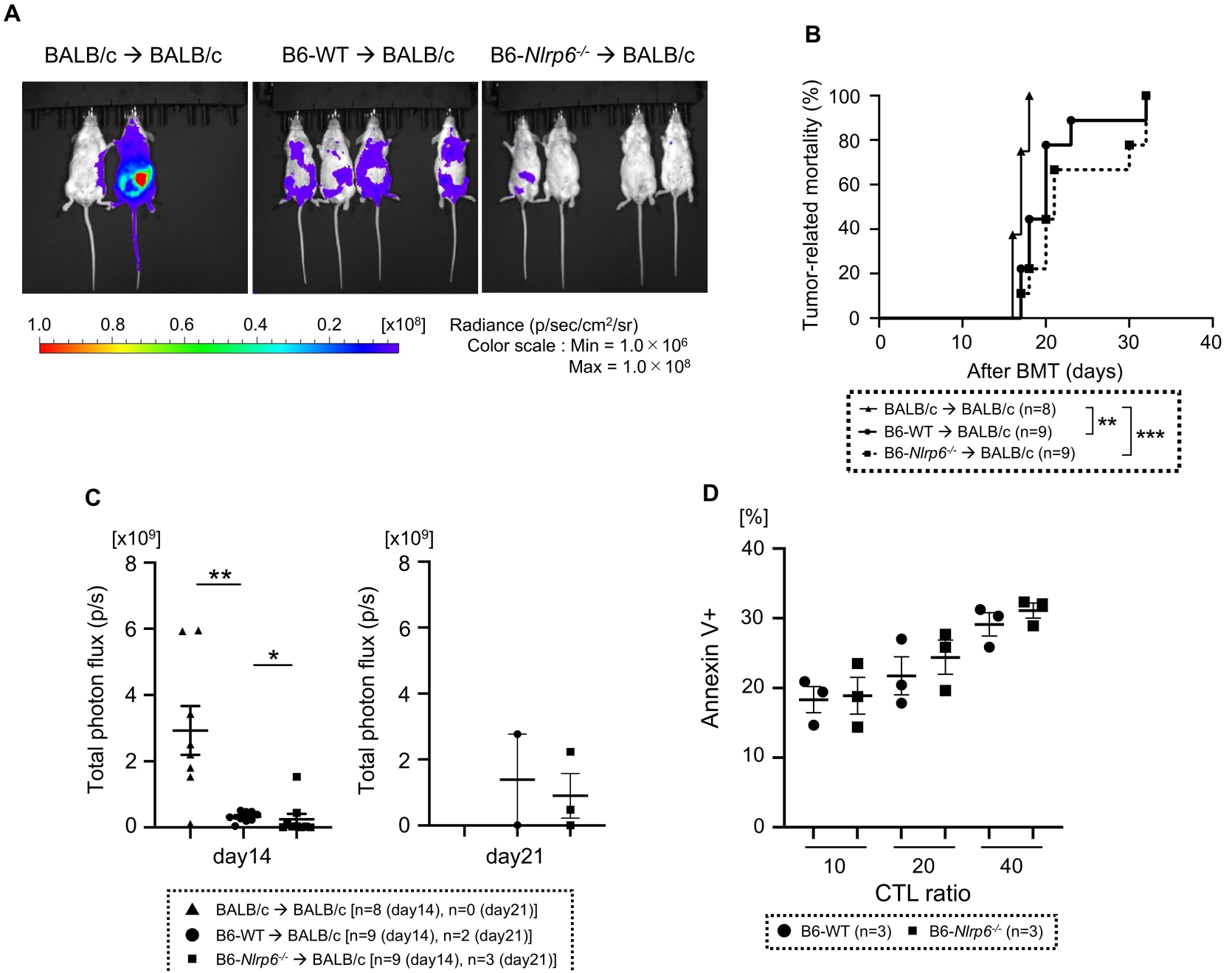
A
BALB/c → BALB/c
B6-WT → BALB/c
B6-Nlrp6-/- → BALB/c
1.0 0.8 0.6 0.4 0.2 [x10^8]
Radiance (p/sec/cm²/sr)
Color scale : Min = 1.0 × 10^6
Max = 1.0 × 10^8
B
Tumor-related mortality (%)
After BMT (days)
BALB/c → BALB/c (n=8)
B6-WT → BALB/c (n=9)
B6-Nlrp6-/- → BALB/c (n=9)
**
***
C
[x10^9]
Total photon flux (p/s)
day14
day21
BALB/c → BALB/c [n=8 (day14), n=0 (day21)]
B6-WT → BALB/c [n=9 (day14), n=2 (day21)]
B6-Nlrp6-/- → BALB/c [n=9 (day14), n=3 (day21)]
D
[%]
Annexin V+
CTL ratio
B6-WT (n=3)
B6-Nlrp6-/- (n=3)

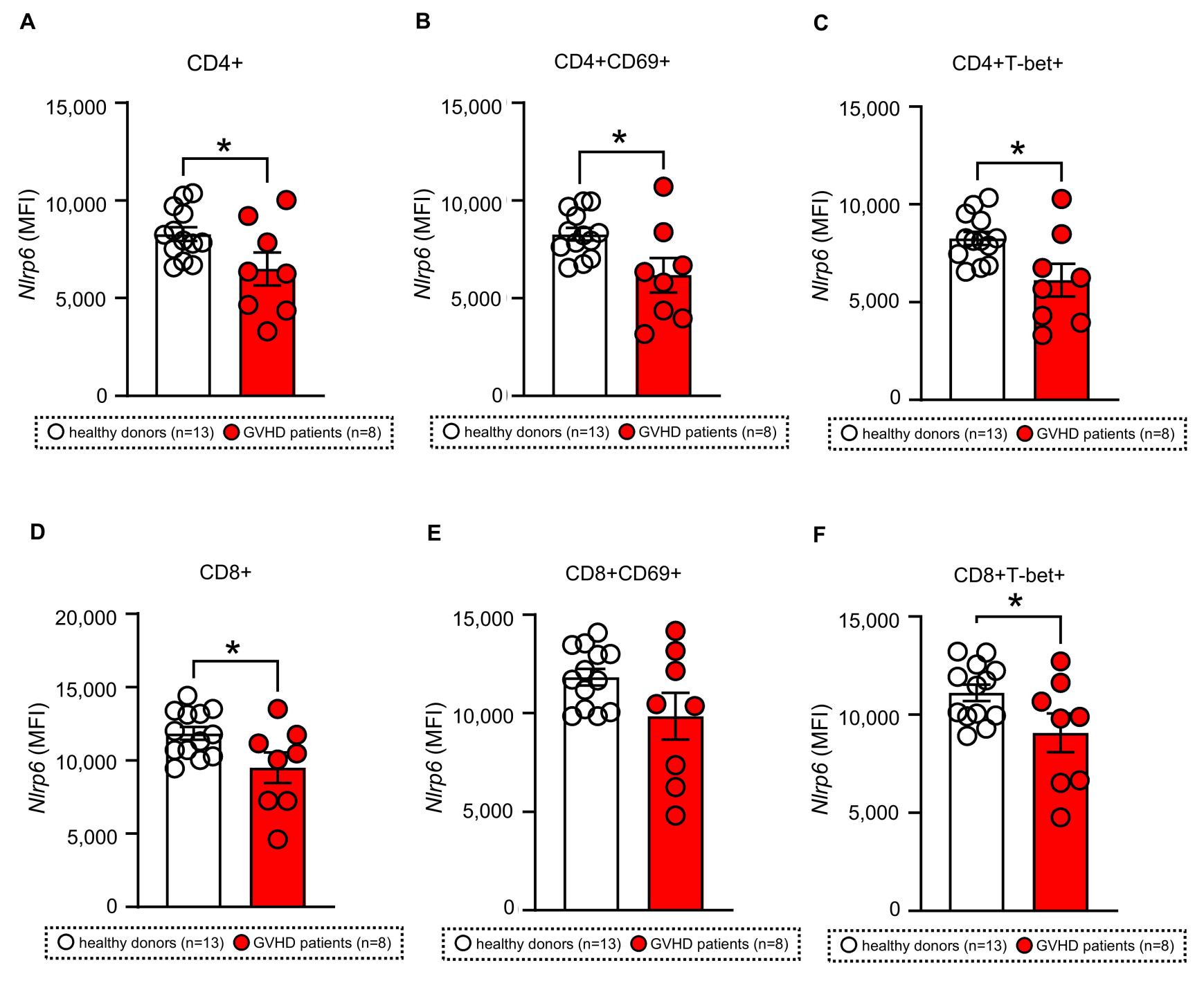
A
CD4+
15,000
10,000
5,000
0
Nlrp6 (MFI)
*
healthy donors (n=13)
GVHD patients (n=8)
B
CD4+CD69+
15,000
10,000
5,000
0
Nlrp6 (MFI)
*
healthy donors (n=13)
GVHD patients (n=8)
C
CD4+T-bet+
15,000
10,000
5,000
0
Nlrp6 (MFI)
*
healthy donors (n=13)
GVHD patients (n=8)
D
CD8+
20,000
15,000
10,000
5,000
0
Nlrp6 (MFI)
*
healthy donors (n=13)
GVHD patients (n=8)
E
CD8+CD69+
15,000
10,000
5,000
0
Nlrp6 (MFI)
healthy donors (n=13)
GVHD patients (n=8)
F
CD8+T-bet+
*
15,000
10,000
5,000
0
Nlrp6 (MFI)
healthy donors (n=13)
GVHD patients (n=8)

Supplemental MATERIALS and METHODS

Mice

C57BL/6 (B6, H-2^b) mice were purchased from the Jackson Laboratory (Bar Harbor, ME, USA) and CLEA Japan, Inc. (Tokyo, Japan). BALB/c (H-2^d) mice were purchased from Charles River Laboratories (Wilmington, MA, USA) and CLEA Japan, Inc. (Tokyo, Japan). B6D2F1 (H-$2^{b/d}$) mice were purchased from the Jackson Laboratory (Bar Harbor, ME, USA) and Japan SLC, Inc. (Hamamatsu, Japan). B10.BR (H-2^k) were purchased from the Jackson Laboratory (Bar Harbor, ME, USA). C3H.sw mice were provided by Mie University, and were bred in our facility. B6 background NLRP6 knock-out (B6-*Nlrp6*$^{-/-}$) mice were provided by Dr. Chen GY[1], the University of Michigan, USA, and were bred in our facility. All age-matched female mice (10-16 weeks old) were used for experiments. All animals were cared for according to regulations reviewed and approved by the University Committee on Use and Care of Animals of the University of Yamagata or University of Michigan, based on the University Laboratory Animal Medicine guidelines. The investigation was conducted in accordance with the Guide for the Care and Use of Laboratory Animals published by the US National Institutes of Health.

RNA extraction and quantitative polymerase chain reaction (PCR)

Total RNA was isolated from stimulated CD90.2+ cells using TRIzol® Reagent (Invitrogen). cDNA was synthesized from 1μg of total RNA using PrimeScript™ RT reagent Kit (TaKaRa Bio Inc, Shiga, Japan) and subjected to quantitative PCR with TB Green® Premix Ex Taq™ II (TaKaRa Bio) on a 7500 Real Time PCR System (Applied Biosystems, Waltham, MA, USA). All reactions were run in triplicate. Samples were normalized to the expression of *Gapdh*. Relative transcript expression of a gene is given as $2^{-\Delta CT}$ ($\Delta C_T = C_{T\ target} - C_{t\ reference}$), and relative changes compared with control are $2^{-\Delta\Delta CT}$ values ($\Delta\Delta C_T = \Delta C_{T\ treated} - \Delta C_{T\ control}$). Sequences of *Nlrp6* primers are forward:5'- CCAGGTGAAGACACTCAGGA-3' and reverse: 5'- TGAGGGTCTTTAGGGAGCATT-3'[1].

In vitro T cell stimulation

Mice CD90.2+ T cells were stimulated at each time point with purified anti-CD3 (1μg/ml; clone 145-2C11, eBioscience, San Diego, CA, USA or Biolegend) and CD28 (1μg/ml; clone 37.51, eBioscience or Biolegend) antibodies. Cells were cultured at 37°C under 5% CO_2 in RPMI 1640 supplemented with 10% fetal calf serum, 1mM sodium pyruvate, 10mM HEPES (4-[2-hydroxyethyl]-1-piperazine-ethanesulfonic acid), 2mM L-glutamine, 10mM HEPES, 1% non-essential amino acids, 100IU/ml penicillin, and 100μg/ml streptomycin (Gibco, Billings, MT, USA).

Bone Marrow Transplantation

BMTs were performed as previously described[2, 3]. Briefly, splenic T cells from donors were enriched, and the bone marrow was depleted of T cells by autoMACS (Miltenyi Biotec) utilizing CD90.2 microbeads (Miltenyi Biotec). We used well-established BMT models. BALB/c, B10.BR, B6D2F1, and C_3H.sw animals were used as recipients and received either 8.5 Gy (^{137}Cs source, BALB/c and B10.BR), 7 Gy (X-ray, BALB/c), 11 Gy (^{137}Cs source or X-ray, B6D2F1), or 10.5 Gy (X-ray, C_3H.sw) on day –1, and 0.5×10^6 (B6→B10.BR), 1×10^6 (B6→BALB/c and B6→C_3H.sw), and 3.5×10^6 (B6→B6D2F1) CD90.2+ T cells along with 5×10^6 T cell-depleted bone marrow (TCD-BM) cells from either syngeneic or allogeneic B6-WT or B6-*Nlrp6*$^{-/-}$ donors on day 0.

BMTs using purified CD4+ or CD8+ T cells were performed in a same manner. BALB/c and C_3H.sw animals were used as recipients and received either 7 Gy (X-ray, BALB/c) or 10.5 Gy (X-ray, C_3H.sw) on day –1, and 0.5×10^6 (B6→BALB/c) and $1\text{-}2\times10^6$ (B6→C_3H.sw) CD4+ or CD8+ T cells along with 5×10^6 T cell-depleted bone marrow (TCD-BM) cells from allogeneic B6-WT or B6-*Nlrp6*$^{-/-}$ donors on day 0.

Non-irradiated B6D2F1 animals received 50×10^6 splenocytes from either syngeneic or allogeneic B6-WT or B6-*Nlrp6*$^{-/-}$ animals[4].

Systemic analysis of GVHD.

We monitored survival after allo-HCT daily and assessed the degree of clinical GVHD (body weight loss, posture, mobility, skin, and fur) weekly as described previously[5]. The investigators were not blinded to allocation during experiments and outcome assessment.

Histopathological analysis of GVHD target organs

GVHD target organs were harvested from recipient mice after allo-BMT, fixed in formalin, embedded in paraffin, sectioned, and stained with hematoxylin and eosin. Histopathological GVHD severity in the gastrointestinal tract was assessed using a semiquantitative scoring system**.** Two independent reviewers evaluated tissue sections in a blinded manner, and the average score was used for analysis.

Post allo-HCT analysis.

BALB/c animals were used as recipients and received irradiation 7Gy (X-ray) on day –1, and 0.5×10^6 CD90.2+ T cells along with 5×10^6 TCD-BM cells from either syngeneic or allogeneic B6-WT or B6-*Nlrp6*$^{-/-}$ donors on day 0. On days 7 and 14, spleens were removed from BMT mice and

analyzed for donor T cell functions (activation and exhaustion markers). In addition, to measure the production of inflammatory cytokine, splenocytes were stimulated with Cell Stimulation Cocktail (1×) (eBioscience) for 4 hours.

Isolation of liver leukocytes.

Livers were harvested from recipient mice after allo-BMT, minced, and mechanically dissociated. The cell suspension was passed through a cell strainer and washed with CMF-PBS containing 5% FBS and 2 mM EDTA. Red blood cells were lysed when necessary, and the recovered cells were stained for flow cytometric analysis.

Bone marrow-derived dendritic cell (BMDC) cultures.

To obtain BMDCs, bone marrow cells from BALB/c mice were cultured with murine recombinant granulocyte-macrophage colony-stimulating factor (20 ng ml^{-1}; PeproTech) for 7 days. BMDCs were isolated by autoMACS (Miltenyi Biotec) utilizing CD11c microbeads (Miltenyi Biotec). They were then utilized as stimulators for mixed lymphocyte reaction (MLR).

Mixed lymphocyte reaction (MLR).

Splenic T cells from B6-WT or B6-*Nlrp6*$^{-/-}$ animals were magnetically separated by MACS using CD90.2 microbeads and used as responders. BMDCs from BALB/c animals were used as stimulators in a mixed lymphocyte reaction. T cells (1×10^5 per well) and irradiated (20 Gy) BMDCs (2.5×10^3 per well) were co-cultured on 96-well U-bottom plates for 96 or 120 hours. The incorporation of ^{3}H-thymidine (1 μCi per well, PerkinElmer) by proliferating T cells during the final 16 hours of co-culture was measured by a Top Count plate reader (Perkin Elmer). When using splenocytes as stimulators, T cells stained with CFSE (4×10^5 per well) were cocultured with irradiated (20 Gy) red blood cell-lysed splenocytes (1×10^5 per well) in 96-well flat-bottom plates for 96 or 120 hours.

CFSE staining.

T cell proliferation was determined with CFSE Cell Division Tracker Kit (BioLegend). Briefly, 2×10^6 cells/ml in PBS with 0.1% BSA (Sigma-Aldrich) were incubated at 37℃ for 20 minutes in a CFSE final concentration of 1 μM, washed two times in RPMI 1640 medium, and placed in cultures.

T cell proliferation assay with BrdU incorporation.

We used the BrdU Flow Kit (BD Biosciences) according to the manufacturer's protocol. CD90.2+ T cells from B6-WT or B6-*Nlrp6*$^{-/-}$ animals were resuspended in RPMI 1640 medium with 10 μM BrdU, and placed in 48 well flat-bottom plates (5×10^5 per well). T cells were incubated for 72 hours after non-specific TCR stimulation. Collected T cells were then stained with surface antibodies, fixed, and permeabilized. Next, T cells were treated with DNase to expose BrdU epitopes, and stained with FITC-conjugated BrdU for 20 minutes at room temperature.

Flow cytometry.

Flow cytometry was performed as previously described[6-8]. Briefly, to analyze T cell surface antigen, splenocytes from transplanted animals or T cells after stimulation *in vitro* were resuspended in 2% fetal bovine serum (FBS, Sigma-Aldrich) in PBS and stained with conjugated monoclonal antibodies (mAbs). The following mAbs were used for surface antigen staining; H2-K^b (FITC: clone AF6-88.5, BioLegend / APC: clone AF6-88.5.5.3, eBioscience, 1:200), CD4 (FITC: clone GK1.5, BioLegend / APC: clone GK1.5, BioLegend / APC-Cy7: clone GK1.5, BioLegend / Pacific Blue: clone GK1.5, BioLegend, 1:200), CD8a (APC: clone 53-6.7, BioLegend / APC-Cy7: clone 53-6.7, BioLegend / Pacific Blue: clone 53-6.7, BioLegend, 1:200), CD25 (APC: clone PC61, BioLegend, 1:200), CD44 (APC: clone IM7, BioLegend, 1:200), CD62L (PE: clone MEL-14, BioLegend, 1:200), CD69 (PE: clone H1.2F3, BioLegend, 1:200), CD107a (LAMP-1) (PE: clone 1D4B, BioLegend, 1:200), and CD366 (Tim-3) (APC: clone RMT3-23, BioLegend, 1:200).

For intracellular staining of cytokines, cytotoxic granules, and transcription factors, cells were stimulated with Phorbol 12-myristate 13-acetate (PMA)/ inonocmysin for 5 hours and then permeabilized with Permeabilization wash buffer (1×) (BioLegend) after surface staining and fixation accoring to the manufacture's protocol. Alternatively, the Foxp3/Transcription Factor Staining Buffer Set (eBioscience) was used according to the manufacture's protocol. The following mAbs were used for staining; FoxP3 (PE: clone MF-14, BioLegend, 1:100), TOX (PE: clone TXRX10, eBioscience, 1:100). IFN-γ (PE: clone XMG1.2, BioLegend, 1:100), T-bet (PE: clone 4B10, eBioscience, 1:100), IL-4 (APC: clone 11B11, eBioscience, 1:100), RORγt (PE: clone B2D, eBioscience, 1:100), IL-17A (APC: clone TC11-18H10.1, BioLegend, 1:100), Granzyme B (PE: clone QA16A02, BioLegend, 1:200), and Perforin (APC: clone S16009B, BioLegend, 1:200).

For intracellular staining to detect T cell receptor signaling molecules, T cells were immediately fixed, washed twice with Permeabilization wash buffer (1×), and stained with NLRP6 (PE: clone 920631, IC9145P, R & D systems, 1:50).

For intracellular staining to detect phosphorylated signaling molecules, T cells were immediately fixed and permeabilized with BD PhosFlow (BD Bioscience) according to the manufacturer's protocol. The following mAbs were used: pErk1/2 (Alexa fluor® 488: clone 20A, BD Bioscience, 1:100), pLck (PE: clone 4/LCK-Y505, BD Bioscience, 1:100), and pSTAT-3 (APC: clone LUVNKLA, eBioscience, 1:100).

For staining early apoptotic cells, T cells were treated with 1x Annexin V Binding Buffer (BD Bioscience) according to the manufacturer's protocol. T cells were stained with Annexin V (APC, BioLegend, 1:100) and Propidium Iodide (PI) (BioLegend, 1:100).

Flow samples were run on a FACS Canto Ⅱ or FACS Melody cell sorter (Becton, Dickinson and Company) and analyzed using FlowJo v10.8.1.

Cytokine ELISA.

Concentrations of TNF and IFN-γ were measured from serum or cell culture supernatant by ELISA with specific anti-mouse mAbs for capture and detection using BD OptEIA (BD Biosciences). Assays were performed according to the manufacturer's protocol and read at 450 nm using a microplate reader (Model xMark^{TM} or 3550; Bio-Rad Labs). All samples and standards were run in duplicate.

T cell differentiation assay.

Naïve CD4+ T cells from B6-WT or B6-*Nlrp6*$^{-/-}$ animals were magnetically separated using CD4 microbeads (Miltenyi Biotec) and resuspended in RPMI 1640 medium. Th1 cells were differentiated using CellXVivo Mouse Th1 Cell Differentiation Kit (CDK018, R&D systems). Naïve CD4+ T cells were resuspended in Differentiation Media and placed in 48 well flat- bottom plates (4×10^5 per well) with anti-CD3 Ab (2 μg/ml). Cells were incubated for 3 days, and transferred to a new plate adding fresh Differentiation Media. Th1 cells were harvested on day 6. Th2 cells were differentiated using ImmunoCult™ Mouse Th2 Differentiation Supplement (STEMCELL). Naïve CD4+ T cells were resuspended in Differentiation Media and placed in 48 well flat-bottom plates (1.5×10^5 per well) with anti-CD3 Ab (1 μg/ml) and anti-CD28 Ab (0.5 μg/ml). On day 2 and 4, cells

were transferred to new plates and incubated with fresh medium. Th2 cells were harvested on day 6. Th17 cells were differentiated using CellXVivo Mouse Th17 Cell Differentiation Kit (CDK017, R & D systems). Naïve CD4+ T cells (3×10^5 per well) were placed in 48 well flat-bottom plates with anti-CD3 Ab (2 µg/ml) and incubated. On day 3, the fresh differentiation medium was added. Th17 cells were harvested on day 5. Differentiated cells were stimulated with Cell Stimulation Cocktail (1×) (eBioscience) for 4 (Th1 and Th2) or 6 (Th17) hours and analyzed for cytokines and transcription factors.

Treg suppression assay.

CD4+CD25- and CD4+CD25+ T cells were isolated from the spleen of WT-B6 or B6-*Nlrp6*$^{-/-}$ animals using CD4+CD25+ Regulatory T Cell Isolation Kit (Miltenyi Biotec) and the autoMACS according to the manufacturer's protocol. CD4+CD25+ T cells were serially diluted from 2×10^4 to 2,500 cells/well and incubated with 2×10^4 CD4+CD25- T cells and 5×10^3 irradiated BALB/c-derived BMDCs for 120 hours. The incorporation of ^{3}H-thymidine (1 µCi/well) by proliferating cells was measured during the last 18 hours of culture.

T-cell signaling assay.

To measure early changes in TCR pathway signaling components, T cells from B6-WT or B6-*Nlrp6*$^{-/-}$ mice were suspended in RPMI 1640 medium at 5×10^6 cells/ml and pre-treated with anti-CD3 Ab (10 µg/ml) and anti-CD28 Ab (5 µg/ml) on ice. Stimulation was started by transferring the cells to a 37 °C water bath for 15 minutes[9]. To measure late changes in signaling, T cells were suspended in RPMI 1640 medium at 1×10^6 cells/ml and incubated in 48 well flat-bottom plates (1×10^6 per well) with anti-CD3 Ab (2 µg/ml) and anti-CD28 Ab (1 µg/ml) at 37°C under 5% CO_2 for the times indicated in the figure legends.

Erk inhibitor treatment.

T cells from B6-WT or B6-*Nlrp6*$^{-/-}$ mice were stimulated with anti-CD3/CD28 antibodies in the presence or absence of the Erk inhibitor. First, 25 mg of FK180204 (Sigma-Aldrich, SML0230-25MG) was dissolved in 7.3673 mL of DMSO to prepare a 10 mM solution. Next, the required volume of 10% RPMI was added to the 10 mM FK180204 to prepare 1 mM and 2 mM FK180204 solutions. 1 mM and 2 mM FK180204 solutions were then added to 100 µL of the T cell solution to adjust the drug concentrations in the respective cell solutions to 10 µM and 20 µM. Each DMSO control sample was adjusted to contain the same amount and concentration of DMSO. After adding the CD3/28 antibody, the cells were incubated at 37°C for 2 and 5 minutes.

Caspase inhibitor treatment.

To examine the effect of caspase inhibition on T cell proliferation and TCR-induced Erk1/2 activation, purified CD90.2+ T cells from B6-WT or B6-Nlrp6-/- mice were treated with Ac-YVAD-cmk (Sigma-Aldrich, SML0429) at a final concentration of 20 μM or with an equivalent concentration of DMSO as a vehicle control. For CFSE-based proliferation assays, CFSE-labeled T cells were seeded at 2×105 cells in 100 μL per well and stimulated with anti-CD3 antibody (4 μg/mL) and anti-CD28 antibody (2 μg/mL) in the presence of Ac-YVAD-cmk or DMSO. CFSE dilution was assessed by flow cytometry after 72 hours of culture.

Western blot analysis.

T cells were lysed in radio-immunoprecipitation assay (RIPA) buffer and total proteins were extracted as previously reported[4, 10]. Equal masses of protein were subjected to 10% sodium dodecyl sulfate-polyacrylamide gel electrophoresis and transferred to polyvinylidene difluoride membranes. Membranes were blocked with 20 mM Tris-HCl, pH 7.4, containing 150 mM NaCl, 0.1% Tween (TBS-T) and 5% milk or 5% bovine serum albumin (BSA). The membranes were probed overnight at 4℃ with the following primary antibodies: Zap-70 (clone 99F2, Cell Signaling Technology, 1:1000), Phospho-Zap-70 (Tyr319) / Syk (Tyr352) (clone 65E4, Cell Signaling Technology, 1:1000), p44/42 MAPK (Erk1/2) (clone 137F5, Cell Signaling Technology, 1:5000), Phospho-p44/42 MAPK (Erk1/2) (Thr202/Tyr204) (clone 197G2, Cell Signaling Technology, 1:1000), and β-tubulin (Cell Signaling Technology, 1:3000). After incubation with horseradish peroxidase-conjugated secondary antibodies diluted in TBS-T containing 5% milk or 5% BSA, immunoreactive bands were detected using Clarity Max Western ECL Substrate (Bio-Rad Laboratories). Images were captured using the Light Capture II system and analyzed using CS Analyzer ver 3.0 software (ATTO, Tokyo, Japan). Protein expression levels were normalized to β-tubulin.

***In vivo* imaging of the GVT effect.**

MHC-mismatched BMT (B6 into BALB/c) was performed as described above except luciferase-transfected Baf/3-ITD tumor cells (500 cells per mouse, provided by Dr. Zeiser, University of Freiburg, Germany) were co-injected. The recipient mice were anesthetized and placed in the dark chamber for image acquisition on days 14 and 21. The tumor cells were imaged by IVIS® Lumina III imaging system (Perkin Elmer). Before imaging, 150 mg/kg of D-luciferin potassium salt solution was intraperitoneally injected into each mouse. After 10 minutes, the mice were

anesthetized with isoflurane and imaged using the IVIS® Lumina III imaging system for 60 seconds.

Cytotoxic T lymphocyte (CTL) assay.

Effector splenic T cells from B6-WT or B6-*Nlrp6*$^{-/-}$ animals were activated by co-culturing them with irradiated (20 Gy) red blood cell-lysed splenocytes from BALB/c mice at a ratio of 5:2 (effector : responder) for 5 days. Activated effector T cells (1×10^5, 2×10^5, or 4×10^5 per well) and target cells (luciferase-transfected Baf/3-ITD tumor cells) (1×10^4 per well) were co-cultured on 96-well U-bottom plates at 37°C under 5% CO_2 for 4 hours. Cells were then washed with Annexin V binding buffer (BD Bioscience) and stained with Annexin V (APC: BioLegend, 1:100) for 15 min at room temperature in the dark. Cells were washed, resuspended in Annexin V binding buffer, and immediately analyzed by flow cytometry.

Spectral flow from human PBMCs.

PBMCs were isolated on the same day as peripheral blood draw using SepMate (Stemcell) according to the manufactures protocol and frozen in 10 % DMSO in FCS. All samples were stained and analyzed in parallel. Viability was analyzed with the Zombie NIR fixable dye. Fc receptors were blocked with anti-human CD16/CD32 (BioLegend) for 15 min at 4 °C, followed by surface staining with fluorochrome-conjugated antibodies for 20 min at 4 °C.

The following ABs were used for surface antigen staining; TIGIT (BUV395: clone 741182, BD 1:40), CD25 (BUV563: clone 2A3, BD 1:50), PD1 (BUV615, clone 612991, BD 1:66), CD3 (Pacific Blue, clone: UCHT1, BioLegend 1:250), CD8 (Spark Blue 550, clone SK1, BioLegend 1:400), CD4 (Spark Blue 547, clone SK3, BioLegend 1:100) CD45 (PerCP, clone: 30-F11, BioLegend 1:100), CD69 (Spark NIR 685, clone FN50 1:40), and Tim-3 (BB700, clone: 344823, BD 1:200).

Cells were fixed and permeabilized for 30 min at 4 °C using the Transcription Factor Staining Buffer Set (eBioscience) for staining of cytoplasmatic proteins and intranuclear proteins. Intracellular markers were stained with fluorochrome-conjugated antibodies for 30 min at room temperature. The following ABs were used for intracellular staining: FoxP3 (Pe-Cy5.5, clone: 236A/E7, BD 1:50), TOX (APC, clone: REA473, Miltenyi 1:50), T-bet (BV711, clone:4B10, BioLegend 1:40), NLRP6 (AF488, clone: 920631, R&D 1:50).
All data were acquired on a SONY full Spectral Analyzer ID 7000 and analyzed with FlowJo v10 (BD).

We obtained written informed consent from all patients prior to analyses. The studies were conducted in accordance with the ethical guidelines of the Declaration of Helsinki and were approved by the Institutional Ethics Review Board of the Medical center, University of Freiburg, Germany (protocol no: 22-1047). Patient characteristics are listed in **Table 1**.

Statistical analysis.

Bars and error bars represent the mean and SEM, respectively. Statistical significance for outocomes other than survival was determined using a two-tailed Mann–Whitney U-test or two-tailed unpaired T-test. A $p<0.05$ was considered statistically significant. We performed survival data analysis using the Log-rank test. All statistical analyses were performed using GraphPad Prism 9. Sample sizes of 3-6 per group were used for *in vitro* studies and 3-20 for individual *in vivo* studies based on our prior experience with these assays. As stated in the figure legends, data were combined from all experiments and shown collectively. All experiments, *in vitro* and *in vivo* were done more than 3 times, in some cases more than four times.

References

1. Chen GY, Liu M, Wang F, Bertin J, Nunez G. A functional role for Nlrp6 in intestinal inflammation and tumorigenesis. J Immunol. 2011;186(12):7187-7194.
2. Reddy P, Maeda Y, Liu C, Krijanovski OI, Korngold R, Ferrara JL. A crucial role for antigen-presenting cells and alloantigen expression in graft-versus-leukemia responses. Nat Med. 2005;11(11):1244-1249.
3. Reddy P, Sun Y, Toubai T, et al. Histone deacetylase inhibition modulates indoleamine 2,3-dioxygenase-dependent DC functions and regulates experimental graft-versus-host disease in mice. J Clin Invest. 2008;118(7):2562-2573.
4. Toubai T, Rossi C, Oravecz-Wilson K, et al. Siglec-G represses DAMP-mediated effects on T cells. JCI Insight. 2017;2(14):
5. Cooke KR, Hill GR, Crawford JM, et al. Tumor necrosis factor- alpha production to lipopolysaccharide stimulation by donor cells predicts the severity of experimental acute graft-versus-host disease. J Clin Invest. 1998;102(10):1882-1891.
6. Toubai T, Fujiwara H, Rossi C, et al. Host NLRP6 exacerbates graft-versus-host disease independent of gut microbial composition. Nat Microbiol. 2019;4(5):800-812.
7. Toubai T, Sun Y, Tawara I, et al. Ikaros-Notch axis in host hematopoietic cells regulates experimental graft-versus-host disease. Blood. 2011;118(1):192-204.
8. Toubai T, Tawara I, Sun Y, et al. Induction of acute GVHD by sex-mismatched H-Y antigens in the absence of functional radiosensitive host hematopoietic-derived antigen-presenting cells. Blood. 2012;119(16):3844-3853.
9. Adachi K, Davis MM. T-cell receptor ligation induces distinct signaling pathways in naive vs. antigen-experienced T cells. Proc Natl Acad Sci U S A. 2011;108(4):1549-1554.
10. Mathewson ND, Jenq R, Mathew AV, et al. Gut microbiome-derived metabolites modulate intestinal epithelial cell damage and mitigate graft-versus-host disease. Nat Immunol. 2016;17(5):505-513.

Supplemental Figure Legend

Supplemental Figure 1. Nlrp6 expression increases early after stimulation.

a-d, B6 WT T cells were stimulated with anti-CD3/28 antibodies *in vitro*. NLRP6 expression was measured by qPCR (n=2-3) (**a**) or flow cytometry (n=4-5) (**c-d**). Representative flow cytometry data are shown in (**b**). Data are shown as the mean ± SEM. %MFI values are expressed relative to the value at 0 minute. All sample numbers are shown in the figure. Statistical significance was analyzed using a two-tailed unpaired T-test (**a**) or a two-tailed Mann-Whitney U-test (**c-d**). **p*<0.05, ** *p*<0.01, ****p*<0.001, *****p*<0.0001.

Supplemental Figure 2. Phenotypic analysis of various T cell subsets and activation markers in naïve B6 WT and *Nlrp6*$^{-/-}$ mice.

Splenocytes were isolated from naïve C57BL6 (B6) WT or *Nlrp6*$^{-/-}$ mice (n=5 per group). Absolute total splenocytes (**a**); the percentages and absolute number of CD4+ and CD8+ T cells (**b**); naïve (CD44-CD62L-), effector memory (EM: CD44+CD62L-), and central memory (CM: CD44+CD62L+) subsets (**c**); activation marker expression (CD25 and CD69) in CD4+ or CD8+ T cells (**d-g**); and regulatory T cells (Treg: CD4+CD25+FoxP3+) (**h**) were measured. Error bars show the mean ± SEM. A two-tailed Mann-Whitney U-test was used for statistical analysis. **p*<0.05.

Supplemental Figure 3. *Nlrp6*$^{-/-}$ donor T cells exacerbate GVHD in the MHC mismatched B6→B10.BR models.

Overall survival of B10.BR mice conditioned with 8.5 Gy TBI on day −1 and transplanted with 0.5×10^6 CD90.2+ splenic T cells along with 5×10^6 TCD-BM cells from allogeneic MHC-mismatched B6 WT or *Nlrp6*$^{-/-}$ donors is shown. n=6-10 per group. Data are pooled from 2 independent experiments.

Supplemental Figure 4. T cell characteristics after MHC-mismatched HCT.

a-l, Recipient BALB/c mice received 7 Gy TBI on day −1 and were transplanted with 0.5×10^6 CD90.2+ splenic T cells from allogeneic MHC-mismatched B6 WT or *Nlrp6*$^{-/-}$ donors along with 5×10^6 TCD-BM cells from WT B6 donors. Splenic T cells or serum cytokines from recipient mice were analyzed on day 7 or day 14 after BMT. **(a)** CD4+ donor T cells (H2-K^b+CD4+), and **(b)** CD8+ donor T cells (H2-K^b+CD8+) are shown. **(c)**The number of activated (CD69+) donor CD4+ and CD8+ T cells are shown. **(d-e)** The number of CD25+ **(d)** and Tim-3+ cells **(e)** in the H2-K^b+CD4+ gate (left) or H2-K^b+CD8+ gate (right) are shown. **(f)** The number of donor CD4+ T cells expressing IFN-γ and T-bet is shown. n=8-9 per group. **(g)** The number of IL-17A+ cells in the H2-K^b+CD4+ gate (left) or H2-K^b+CD8+ gate (right) are shown. n=4-7 per group. **(h)** The number of allogeneic donor Tregs (H2-K^b+ CD25+FoxP3+) is shown. n=6-8 per group. **(i)** The serum levels of TNF-α on day 7 is depicted. n=3-7 per group. **(j-l)** Expansion of donor T cells in MLNs was measured. Whole T cells **(j)**, CD4+ T cells **(k)**, and CD8+ T cells **(l)** in MLNs are shown. n=3-6 per group.

Data are pooled from 2-3 independent experiments. Statistical significance was determined using a two-tailed Mann-Whitney U-test (**a-l**). **p*<0.05, ***p*<0.01. Data are shown as the mean ± SEM. All sample numbers are described in the figure.

Supplemental Figure 5. Effect of caspase inhibition on T cell proliferation.

T cells from B6-WT or *Nlrp6*$^{-/-}$ mice were stimulated with anti-CD3/CD28 antibodies in the presence of a caspase inhibitor (Ac-YVAD-cmk) or DMSO control. For CFSE-based proliferation assays, Ac-YVAD-cmk or DMSO was added at the start of culture, and CFSE dilution was analyzed after 72 hours.

Supplemental Figure 6. The absence of NLRP6 enhances Zap-70 and Erk phosphorylation.

a-b, Spleen T cells from either B6 WT or *Nlrp6*$^{-/-}$ mice were stimulated with anti-CD3/28 antibodies for 6 hours. Downstream signal transduction components of T cell receptor signaling were measured by western blot. Representative images of pZap-70 (**a**) and pErk1/2 (**b**) are shown. In addition, the pZap/Zap-70 (**c**) and pErk/Erk ratios (**d**) were calculated. (**e**) T cells from either B6 WT or *Nlrp6*$^{-/-}$ mice were stimulated with anti-CD3/28 antibodies for 2-5 minutes. MFI (left panel) and %MFI values are expressed relative to the value at 0 minute in CD4+ or CD8+ T cells (right panel) are shown.

(f) T cells from either B6 WT or *Nlrp6*$^{-/-}$ mice were stimulated with anti-CD3/28 antibodies for 2 minutes in the presence of an Erk kinase inhibitor (FR180204, 10 μM). Phosphorylated Erk1/2 was then measured by flow cytometry (n=4). Representative histograms of control (grey) and 2 minutes after stimulation (WT-T cells: blue or *Nlrp6*$^{-/-}$ T cells: red) are shown (left panel). Percentage of pErk1/2+ cells in CD4+ or CD8+ T cells are shown (n=4, right panel). (**g**) T cells from either B6 WT or *Nlrp6*$^{-/-}$ mice were stimulated with anti-CD3/28 antibodies for 2 minutes in Erk inhibitor-contained media. Erk inhibitor was added to media at a concentration of 10 μM or 20 μM. Phosphorylated Erk1/2 was then measured by flow cytometry. Percentage of pErk1/2+ cells in CD4+ or CD8+ T cells are shown (n=4). Statistical significance was determined using a two-tailed Mann-Whitney U-test (**e-g**). *p<0.05. Data are shown as the mean ± SEM.

Supplemental Figure 7. NLRP6 does not affect phosphorylation of Lck or Stat3.

a-b, T cells from either B6 WT or *Nlrp6*$^{-/-}$ mice were treated with anti-CD3/28 antibodies for 5-60 minutes or 6-24 hours. Phosphorylation of Lck (**a**) and Stat3 (**b**) were measured by FACS (n=3-4). A two-tailed Mann-Whitney U-test was used to determine statistical significance. Data are shown as the mean ± SEM.

Supplemental Figure 8. GVT responses of *Nlrp6*$^{-/-}$ and WT T cells to Baf/3-ITD leukemia cells were equivalent.

B6 WT or *Nlrp6*$^{-/-}$ CD8+ T cells were collected after bulk MLR and CD107a (**a**), Granzyme B (**b**), and Perforin (**c**) expression were measured by flow cytometry (n=4). Statistical significance was analyzed using the two-tailed Mann-Whitney U-test. Data are shown as the mean ± SEM.

Supplemental Figure 9. NLRP6 expression is reduced in T cells of aGVHD patients.

PBMCs of healthy donors (n=13) and aGVHD patients (n=8) were analyzed by spectral flow. MFI of NLRP6 was evaluated on multiple T cell subsets. Normality was assessed using the Shapiro-Wilk test. Statistical significance was analyzed using a two-tailed unpaired T-test (**a-f**). *p<0.05. Data are shown as the mean ± SEM. All sample numbers are shown in the figure.

Supplemental Figure 1

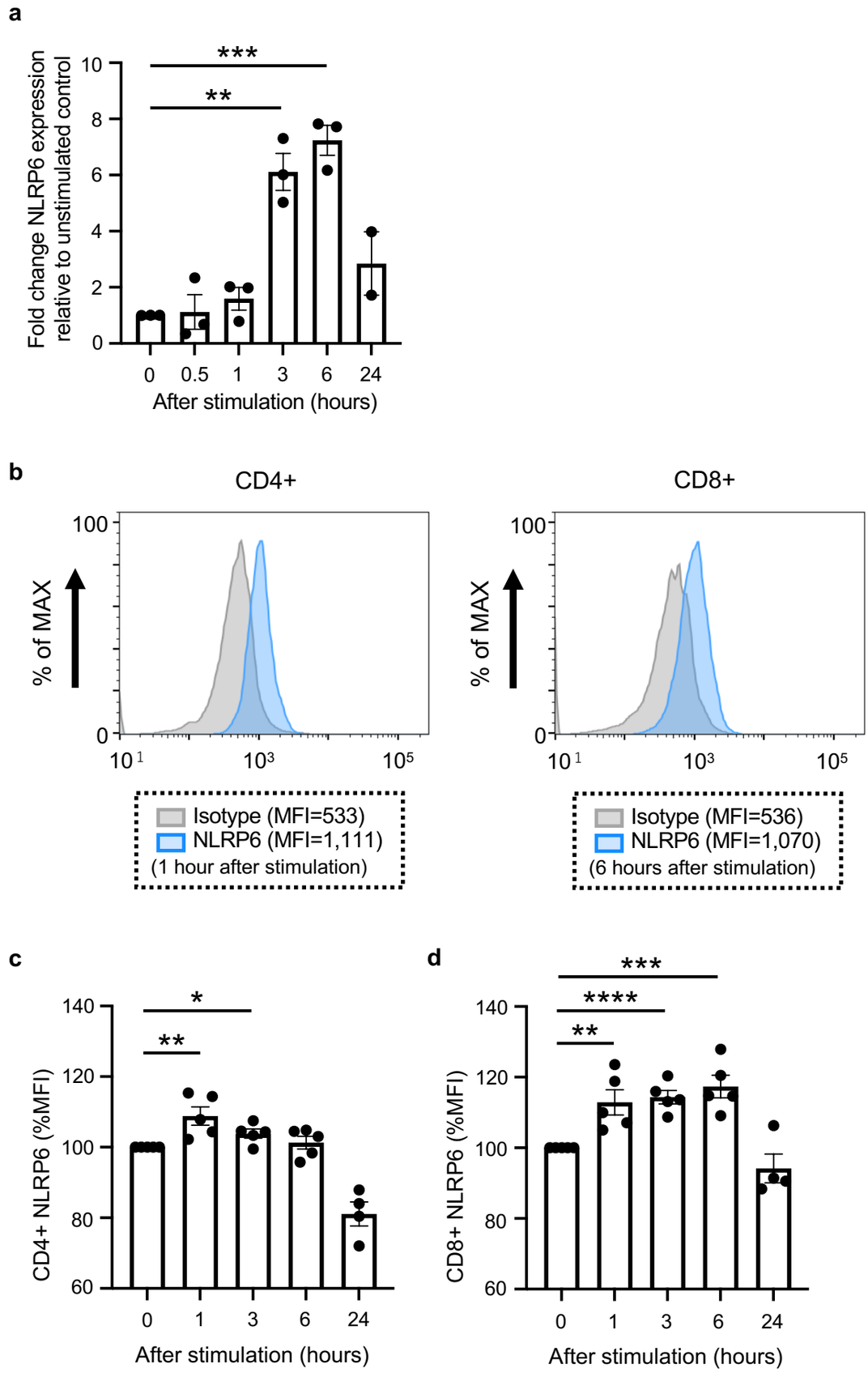

Supplemental Figure 2

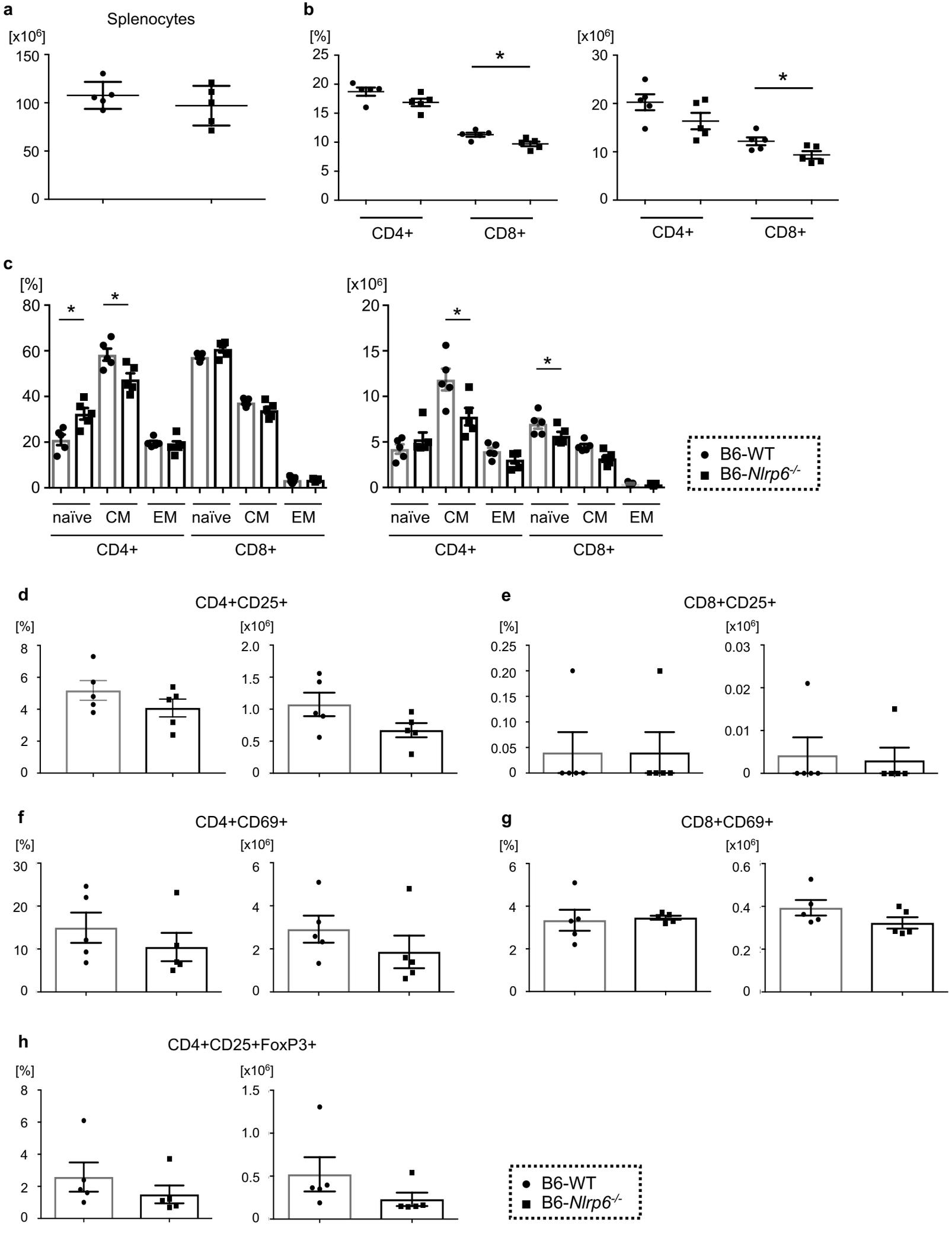

Supplemental Figure 3

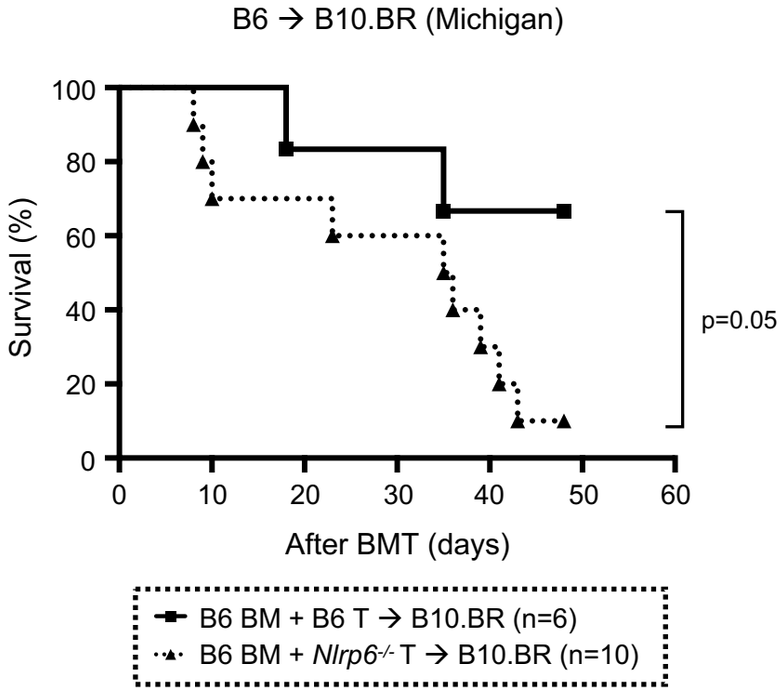

Supplemental Figure 4

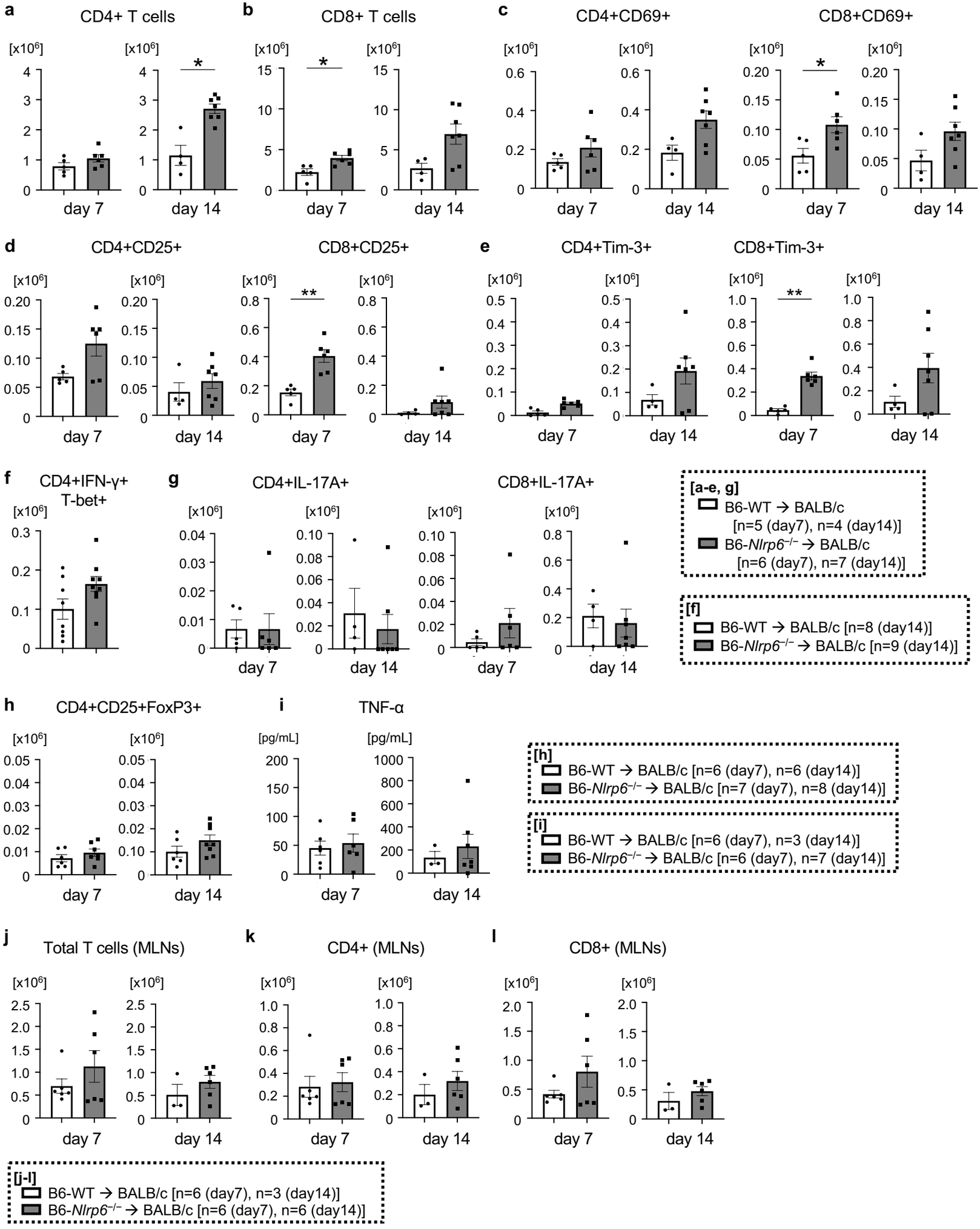

Supplemental Figure 5

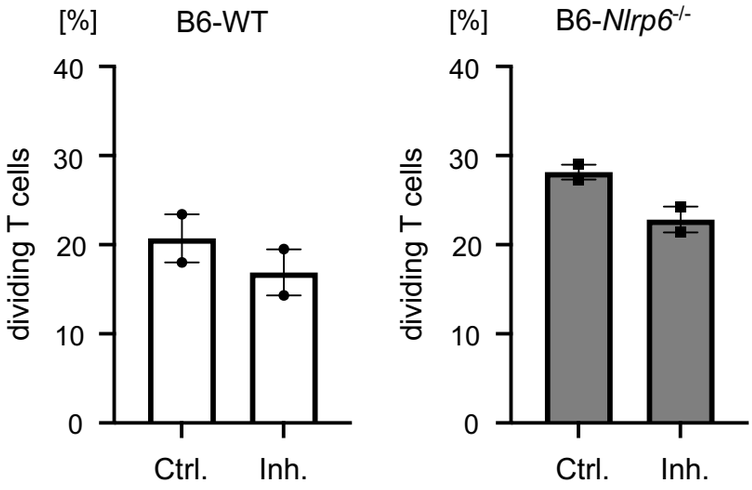

Supplemental Figure 6

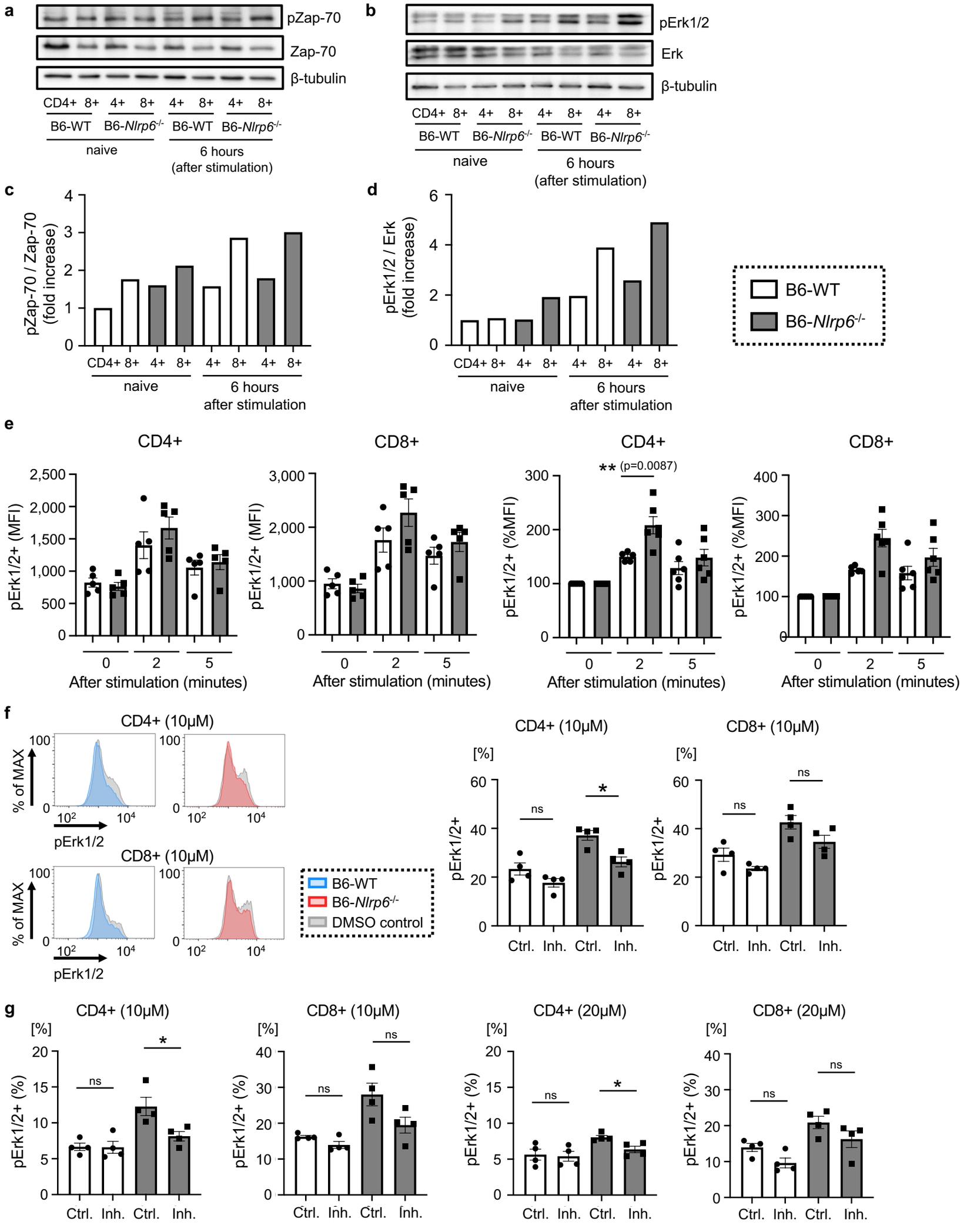

Supplemental Figure 7

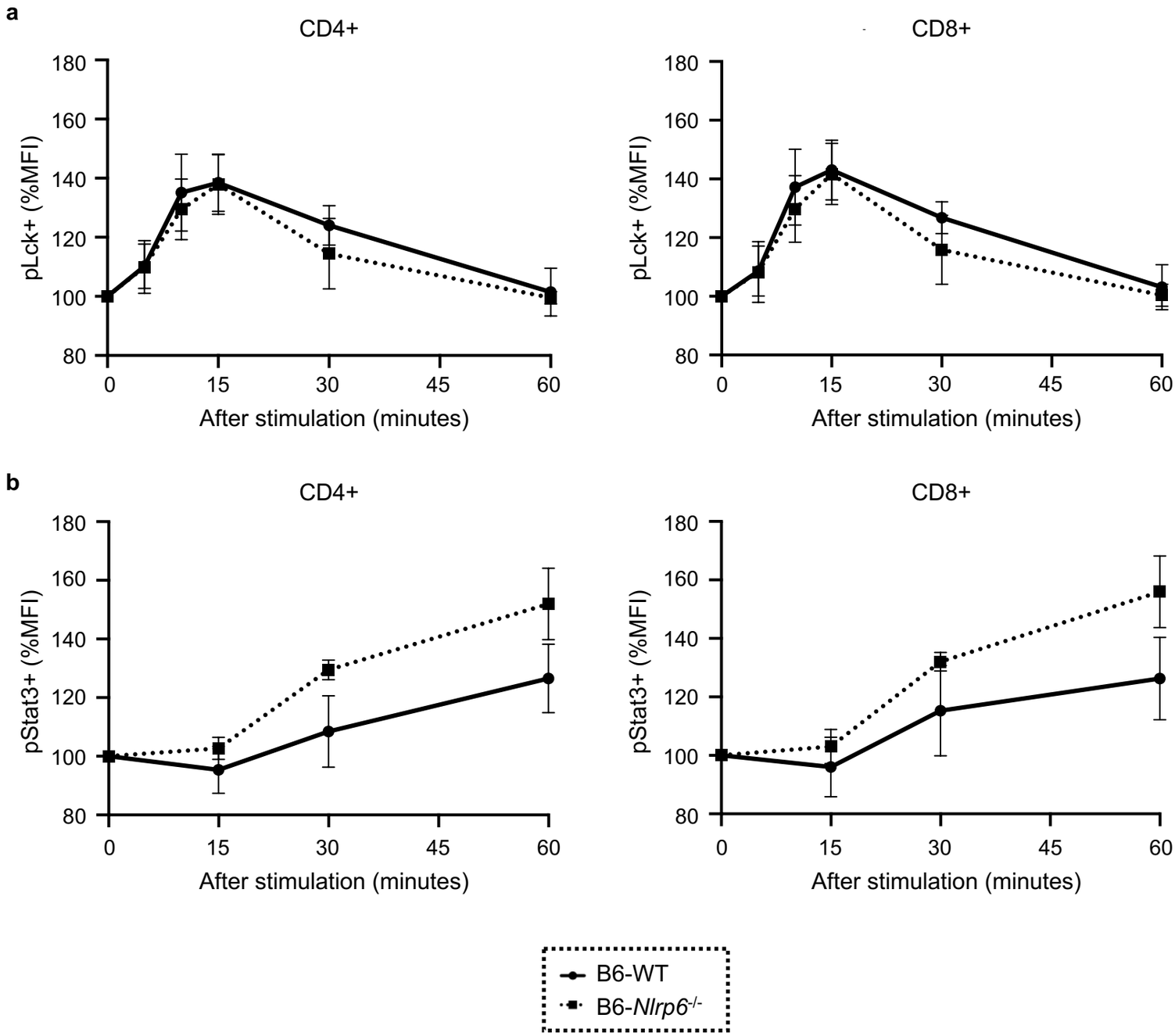

Supplemental Figure 8

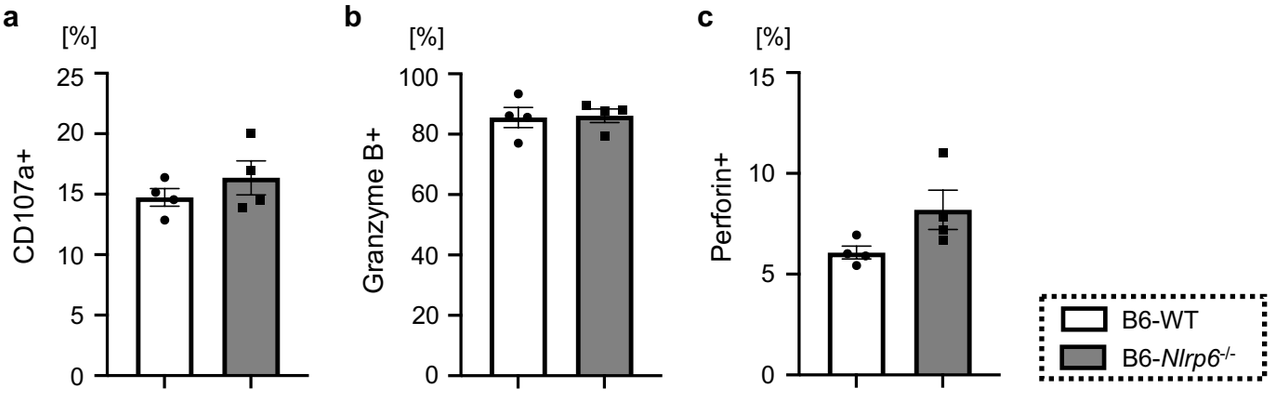

Supplemental Figure 9

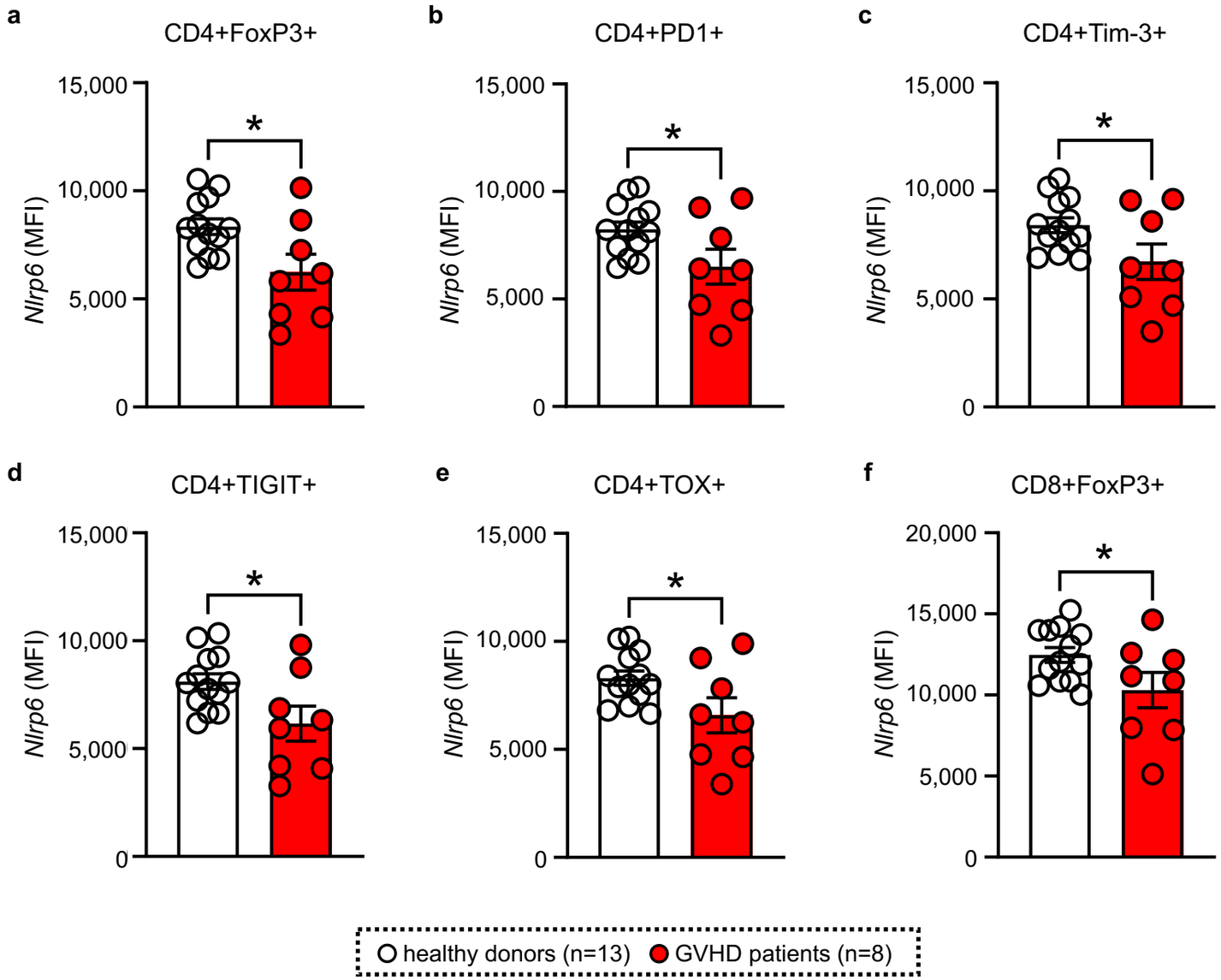

Supplemental Table 1

	Cohort	GVHD patients
	No. of patients	8
	Age at HCT, years	54.8 (27.0–72.6)
Sex	male	3
	female	5
Primary diagnosis	AML	4
	ALL	2
	MDS	2
Conditioning regimen	RIC	3
	MAC	5
Donor type	HLA-identical	5
	HLA-mismatched	3
Graft source	PBSC	8
	BM	0
CMV serostatus	Positive	3
	Negative	5
Overall GVHD grade	2	3
	3	4
	4	1
GVHD prophylaxis	CyA/MMF	1
	CyA/MMF/ATG	3
	CyA/MMF/Cyclophosphamide	3
	CyA/EC-MPS/ATG	1
Immunosuppression	None	1
	Prednisolone	4
	Prednisolone + Ruxolitinib	2
	Prednisolone + Ruxolitinib + Budesonide	1
Sampling	Days after GVHD diagnosis	20 (0–78)

	Cohort	Healthy controls
	No. of patients	13
	Age, years	41.88 (28.0–67.6)
Sex	male	6
	female	7